# MULTIPLE MILANKOVITCH CYCLES IN THE BRIDGE CREEK LIMESTONE (CENOMANIAN-TURONIAN), WESTERN INTERIOR BASIN

B.B. SAGEMAN[1], J. RICH[1], M.A. ARTHUR[2], W.E. DEAN[3], C.E. SAVRDA[4], AND T.J. BRALOWER[5]

[1]*Department of Geological Sciences, Northwestern University, Evanston, Illinois, 60208*

[2]*Department of Geosciences, Penn State University, University Park, Pennsylvania, 16802*

[3]*U.S. Geological Survey, MS 980, Federal Center, Denver, Colorado, 80225*

[4]*Department of Geology, Auburn University, Auburn, Alabama, 36849*

[5]*Department of Geology, University of North Carolina, Chapel Hill, North Carolina, 27599*

ABSTRACT: Spectral analyses of complementary lithologic and paleoecologic data sets from the Cenomanian-Turonian Bridge Creek Limestone are used to test for Milankovitch periodicities. Because the analyses quantitatively assess variance in the data sets through the study interval, they also offer a new method for evaluating relationships between different components of the depositional system. The analysis was made possible by high-resolution sampling for geochemistry, ichnology, and microfossils from a complete section of the Bridge Creek Limestone Member in the USGS #1 Portland core, coupled with a detailed chronostratigraphic framework established for the interval in a recently published compilation of new radiometric dates and biozones. The analyzed data included weight percent carbonate (% $CaCO_3$) and organic carbon (% OC), grayscale pixel values, ichnologic measures such as maximum burrow diameter and ichnocoenosis rank, and relative abundance values for selected nannofossil taxa. The lithologic parameters produced significant spectral responses for all three major orbital cycles (eccentricity, obliquity, and precession) in the upper 6 meters of the study interval. Spectra for ichnologic data are similar to those for % OC, possibly because both of these variables are dominantly controlled by benthic redox conditions. Spectra for some nannofossil taxa show results similar to % OC or % $CaCO_3$ but are less definitive due to preservational effects. A new model to explain the Bridge Creek cycles is developed based on the spectral results. The model combines dilution and productivity mechanisms by suggesting that obliquity predominantly forces dilution through its effect on high-latitude precipitation, whereas precession predominantly forces carbonate productivity through its effect on evaporation and nutrient upwelling in the Tethyan realm to the south. The two influences mix in the shallow Western Interior epicontinental basin, where they result in constructive and destructive interference (because of the different frequencies of obliquity and precession) to produce the complex bedding pattern observed in the Bridge Creek Limestone.

## INTRODUCTION

In recent years Fourier techniques have been successfully employed to quantify evidence for Milankovitch forcing in sedimentary records of pre-Pleistocene strata (e.g., Park and Herbert, 1987). However, they have not been applied to the rhythmically bedded Cretaceous strata of the Greenhorn Formation, Western Interior basin, from which Gilbert (1895) first proposed the theory of climatic forcing of sedimentary rhythms. In this paper we report evidence of Milankovitch periodicities in the Bridge Creek Limestone Member of the Greenhorn Formation, obtained by applying Fourier techniques to lithologic and paleontologic data. The study was made possible by recent refinements in chronostratigraphy (Obradovich, 1993; Kauffman et al., 1993), and the collection of continuously sampled, high-resolution stratigraphic, paleontologic, and geochemical data sets from a core drilled in central Colorado (Dean and Arthur, this volume). These data include lithologic variations quantified in measured sections and core photographs, variations in measured contents of carbonate (% $CaCO_3$) and organic carbon (% OC) of the rocks (Sageman et al., 1997), variations in ichnologic characteristics observed in the core (Savrda, this volume), and changes in nannofossil assemblages analyzed in core samples (Burns and Bralower, this volume).

Variations in % $CaCO_3$ and % OC of pelagic and hemipelagic strata commonly are interpreted to reflect the interplay between clastic dilution, primary production, carbonate dissolution, and bottom-water oxygen content, factors that may be influenced or controlled by climate cycles (Arthur et al., 1984). These data were successfully employed in spectral estimates of Milankovitch forcing in Italian limestone/marlstone cycles (Park and Herbert, 1987). Variations in trace-fossil content provide an independent assessment of changes in benthic redox and substrate conditions (Savrda and Bottjer, 1991), and were successfully employed recently in spectral analyses of Cretaceous limestone/marlstone sequences (Erba and Premoli-Silva, 1994). Changes in the relative abundance of nannofossil species are interpreted to reflect water-mass conditions in the Western Interior basin, including surface-water temperature, salinity, and nutrient supply (Watkins, 1985; Bralower, 1988; Roth and Krumbach, 1988; Watkins et al., 1993). These parameters are also potentially sensitive to climate cycles (Watkins, 1989), but relative abundance trends in Cretaceous nannofossils of the Western Interior have not been tested with spectral techniques.

In this study we analyzed independent lithologic and paleontologic data sets of the Bridge Creek Limestone for Milankovitch periodicities. The results represent the first spectral evaluation of periodic oscillations corresponding to the Milankovitch precession, obliquity, and (or) eccentricity frequencies in the stratal patterns of the Bridge Creek Limestone. What is most significant about the study, however, is the simultaneous spectral analysis of three independent data records that are interpreted as largely reflecting sedimentation processes, benthic redox and substrate conditions, and surface-water conditions. Comparing results among the different data sets allows independent assessments of the mechanisms for sedimentary expression of orbitally influenced climate cycles. These results are helpful in evaluating different models for the linkage between climate and depositional systems in the Northern Hemisphere during Cenomanian-Turonian time.

Stratigraphy and Paleoenvironments of the Cretaceous Western Interior Seaway, USA, SEPM Concepts in Sedimentology and Paleontology No. 6

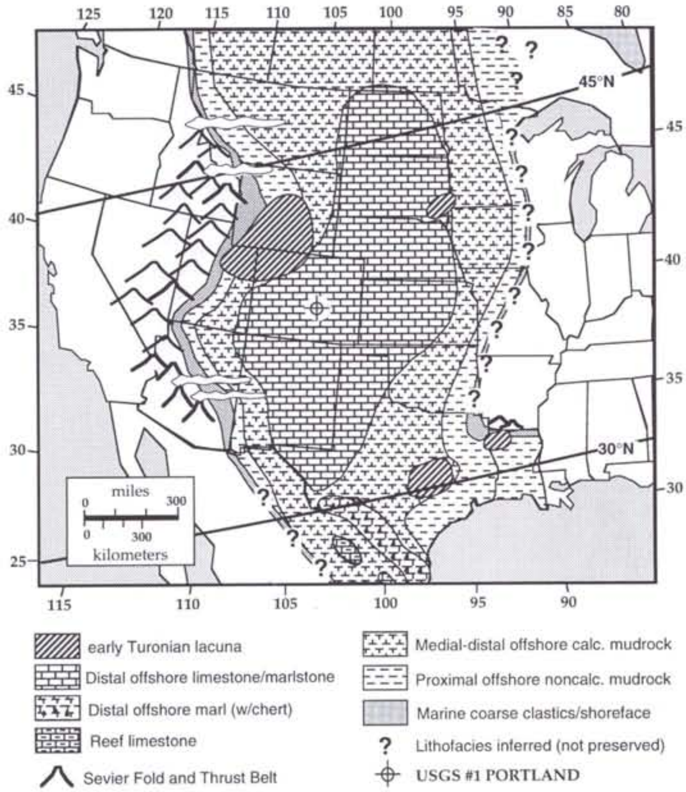


FIG. 1. Locality map shows the site of the Portland core in relation to paleogeography and the distribution of lithofacies for the Western Interior Basin during Early Turonian time (*Watinoceras devonense* Biozone).

## GEOLOGICAL BACKGROUND

The history of the Western Interior basin of North America (Fig. 1) is well documented in several recent compilations (Pratt et al., 1985; Caldwell and Kauffman, 1993; Caputo et al., 1994). Aspects of this history relevant to our study include the paleogeography, climatic history, sedimentology, and oceanography of the seaway during deposition of the Bridge Creek Limestone. At this time, (during the Late Cenomanian to Early Turonian), a combination of foreland-basin subsidence and tectono-eustatic highstand resulted in maximum flooding of the Western Interior basin (Jordan, 1981; Kauffman, 1984). As a result, a meridional seaway formed that extended across more than 30° of latitude, connecting the circumpolar ocean to the western Tethys (Kauffman, 1977, 1984). Thus, the basin spanned both the lower latitude zone of high evaporation as well as the higher latitude precipitation belt (inferred from generalized modern atmospheric circulation patterns). Climatic interpretations from geologic data suggest warm temperate to subtropical climates with humid to subhumid conditions for the central Western Interior region (Kauffman, 1984; Pratt, 1984; Upchurch and Wolfe, 1993; Ludvigson et al., 1994; Witzke and Ludvigson, 1994). In addition, general circulation model experiments to analyze the effects of orbitally forced changes in insolation suggest that monsoonal circulation intensified in northern mid-latitudes and led to periodic fluctuations in the hydrologic cycle (Glancy et al., 1993; Park and Oglesby, 1991, 1994).

Sedimentation was dominated by abundant siliciclastic input from the uplifted fold and thrust belt to the west, but comparatively little clastic sediment from the east (Kauffman, 1984). Deposition of the Bridge Creek Limestone began just prior to and spanned one of the peak highstand events in the basin. Sedimentation was characterized by oscillations between mud-rich and carbonate-rich facies that ultimately formed limestone/marlstone bedding couplets. These couplets are characterized by fluctuations in biofacies and organic carbon content that are interpreted by many (e.g., Barron et al., 1985) to reflect changes in bottom-water oxygen content. The most common oceanographic model for circulation in the Western Interior basin during Late Cenomanian to Early Turonian time proposes fluctuations between a stratified and mixed water column to explain the benthic redox cycles (Barron et al., 1985; Pratt et al., 1993). Proponents of this hypothesis contend that the lithologic and interpreted redox characteristics of the Bridge Creek couplets are accounted for by changes in clastic dilution and water column stratification, respectively, due to Milankovitch forcing of precipitation and runoff. Alternate hypotheses were proposed for productivity as the dominant mechanism in forming the carbonate-rich units (Eicher and Diner, 1985, 1989, and 1991; Ricken, 1991, 1994) and for the combined influence of dilution and productivity (Arthur and Dean, 1991).

Previous investigators evaluated the Milankovitch hypothesis for the Bridge Creek Limestone, typically using bed counts and established time scales to estimate the periodicity of the bedding couplets. Kauffman (1977) used radiometric data from Obradovich and Cobban (1975) to estimate bedding periodicity at 60-80 ky. Fischer (1980) calculated periodicities of 27 to 22 ky and later revised that estimate to 41 ky (Fischer et al., 1985) based on additional data collected by Pratt (1984). Elder (1985) identified prominent limestone beds in the Bridge Creek sequence, and using Kauffman's (1977) time scale, estimated periods of 100 ky for them. Many authors cite a range between 20 and 40 ky for the lithologic couplets (e.g., Arthur et al., 1984; Arthur and Dean, 1991), or simply offer 40 ky as the average between minimum and maximum published estimates (Barron et al., 1985; Pratt, 1985; Pratt et al., 1993). Two recent studies illustrate the continued lack of resolution in periodicity estimates of the Bridge Creek bedding cycles. Based on analysis of ichnofossils in a core of the Bridge Creek Limestone drilled near Pueblo, Colorado, Savrda and Bottjer (1994) found that the thickest limestone beds in the lower part of the Bridge Creek, which correspond to the limestone marker beds of Cobban and Scott (1972), contain the largest and deepest burrows, and assigned these the highest values for their oxygen-related ichnocoenoses (ORI) index. However, between these bioturbated beds (presumably representing the highest oxygen levels), they found bundles of four to six ORI cycles of lower degrees of bioturbation (presumably representing lower oxygenation levels) that were not manifested as obvious lithologic variations. Savrda and Bottjer interpreted these cycles as evidence of 20-ky precessional cycles (smaller ORI cycles) within the predominant 100-ky eccentricity cycles (major limestone beds). Kauffman (1995) analyzed lithologic couplets defined in the Rock Canyon outcrop section and using Obradovich's (1993) new radiometric dates, calculated a period of 41 ky for the bedding couplets and 100 ky for intervals bounded by "prominent" (i.e., thicker) limestones. These varied interpretations illustrate the difficulties inherent in defining couplets based on different parameters as well as the problems that stem from age uncertainties. With the recent improvements in radiometric dating of the Late Cenomanian to Early Turonian interval (Obradovich, 1993), time series analysis of data from a con-

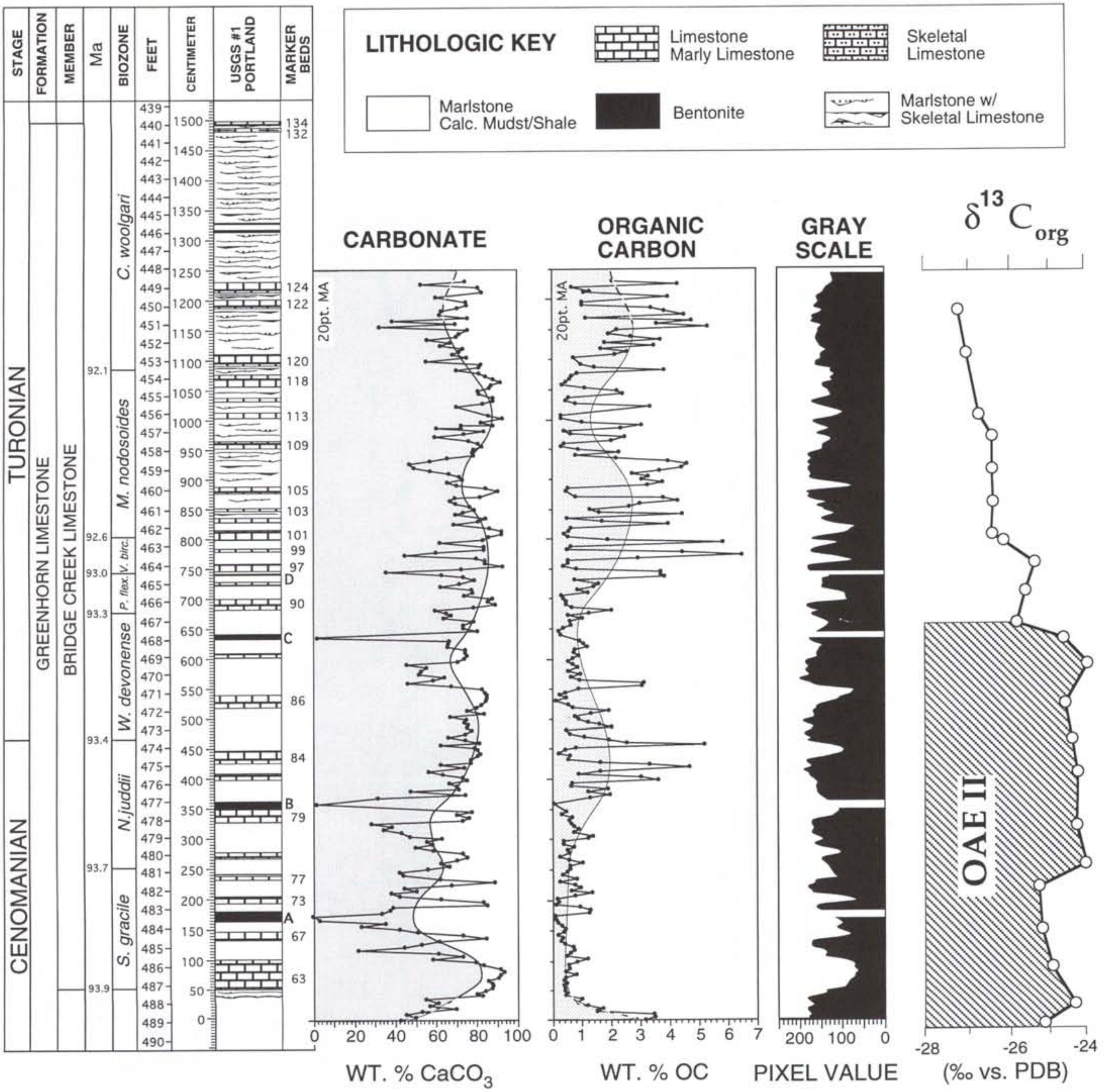


FIG. 2. Lithologic section of the Portland core plotted with weight % $CaCO_3$, weight % OC, and gray-scale pixel values (darker values increase to the left). Plot of $\delta^{13}C$ organic matter (Pratt, 1985) defines OAE II. Depths are given in feet below the top of the core, and in centimeters above a core break in the Hartland Shale Member just below the base of the Bridge Creek Limestone Member (487.5 ft). Shaded regions in $CaCO_3$ and OC plots show 20-point moving averages (MA). Marker bed numbers of Cobban and Scott (1972) and bentonites A-D of Elder (1985) indicate correlations to the Rock Canyon Anticline reference section. Radiometric ages are based on the Kauffman et al. (1993) time scale. Biozonation from Kennedy and Cobban (1991).

tinuous core offers a means to more objectively and quantitatively test for periodicities in the Bridge Creek Limestone Member.

## METHODS

The Portland core was acquired as part of the Cretaceous Western Interior Seaway Drilling Project (Dean and Arthur, 1994, and this volume). At the drill site Cretaceous strata of interest are horizontal and structurally undisturbed, which allowed total recovery of the core (Dean and Arthur, this volume). High-resolution lithologic description and measurement of the Portland core was completed by Arthur and Sageman following collection and curation by the USGS Core Research Center in Denver, CO (Dean and Arthur, this volume). The Bridge Creek Limestone interval is illustrated in Figure 2. Marker beds defined by

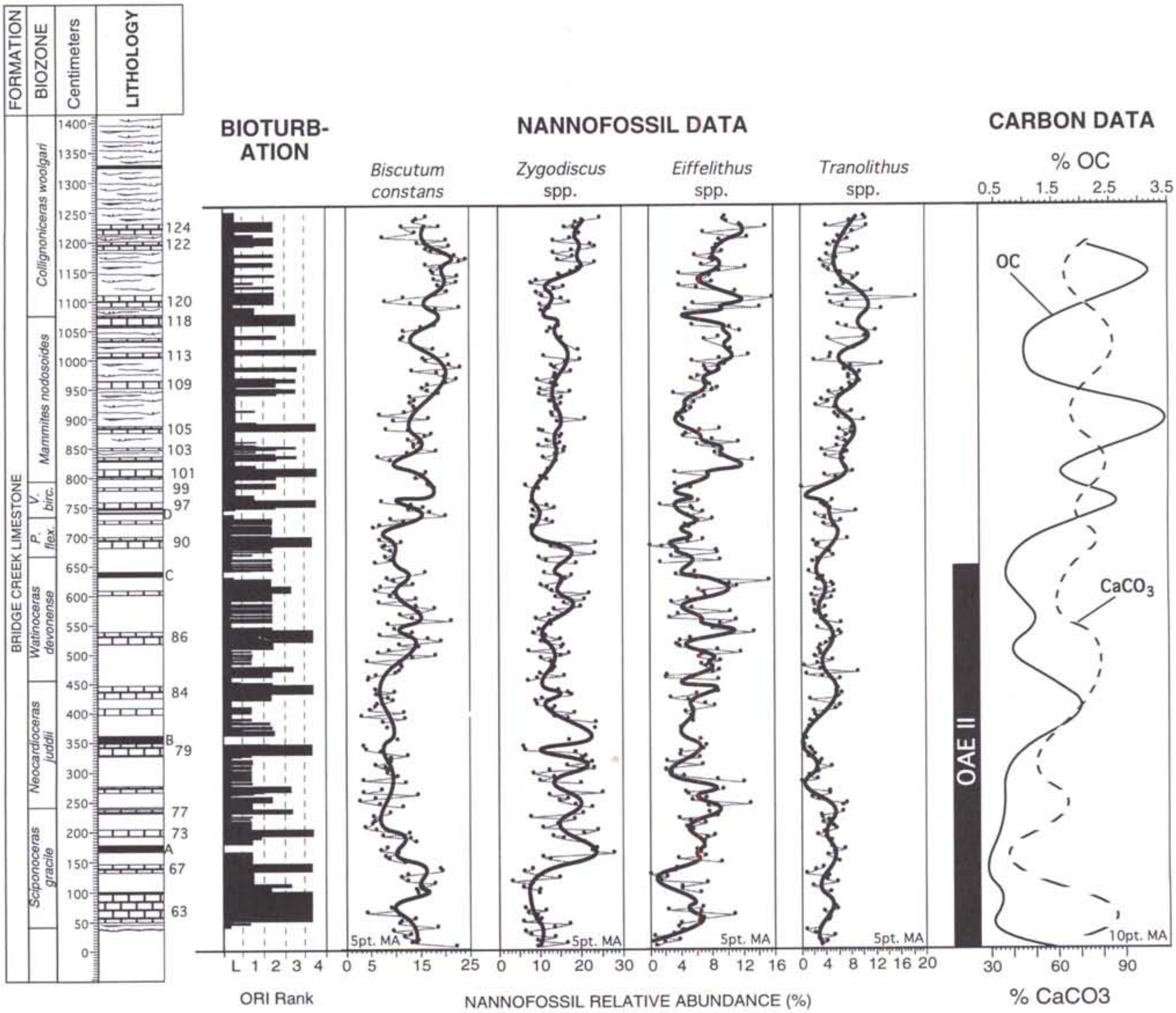


FIG. 3. Lithologic section of USGS #1 Portland core plotted with oxygen-related ichnocoenosis rank values (ORI) and relative abundance data (percent of assemblage) for four nannofossil taxa. Shown for comparison are 10-point moving average (MA) curves of % $CaCO_3$ and % OC data, as well as a black bar indicating OAE II.

Cobban and Scott (1972) and Elder (1985) were identified in the core by correlating to the Cretaceous reference section at Rock Canyon Anticline (which is approx. 40 km east of the drill site) where these beds were first recognized. The boundaries of standard Western Interior ammonite biozones (Cobban, 1984, 1985; Elder, 1985; Kennedy and Cobban, 1991) were defined for the core based on the lithologic correlations (Fig. 2).

*Lithologic Data*

To quantify lithologic variations through the 12.5 m of well-developed limestone-marlstone bedding couplets in the study interval, 1-cm-thick samples were taken at 5-cm intervals and analyzed for carbon content. The samples were crushed to <200 mesh and analyzed by coulometry (Engleman et al., 1985). The carbonate in the untreated whole samples was acidified with perchloric acid to liberate $CO_2$, which was titrated in the coulometer cell to measure carbonate carbon. Total carbon was measured by titrating $CO_2$ that was liberated during sample combustion at 950$^{\circ}$ C in a stream of oxygen. The technique has a precision of better than ± 0.5% for both carbonate and total carbon. Organic carbon (OC) was calculated as the difference between total and carbonate carbon, and % $CaCO_3$ was calculated based on stoichiometry. Samples within altered volcanic ash (bentonite) beds were removed from the time series prior to spectral analysis. Because of slight irregularities in lithology and core recovery, some of the sample intervals varied up to 1 or 2 cm. A cubic spline was applied to the slightly unevenly spaced

TABLE 1.- *Effective sedimentation rates for selected biozones of the Greenhorn Limestone.*

| | Age at base | Duration | Thickness | S | |
|---|---|---|---|---|---|
| Biozone | Ma | My | m | My/m | cm/ky |
| base Fairport Chalky Shale | 91.90 | | | | |
| *C. woolgari (part)* | 92.10 | 0.20 | 4.20 | 0.05 | 2.10 |
| *M. nodosoides* | 92.60 | 0.50 | 2.80 | 0.18 | 0.56 |
| *W. devonense-V. birchbyi* | 93.40 | 0.80 | 3.40 | 0.24 | 0.42 |
| *N. juddii* | 93.70 | 0.30 | 2.10 | 0.14 | 0.70 |
| *S. gracile* | 93.90 | 0.20 | 2.05 | 0.10 | 1.02 |
| *D. conditum* | 94.18 | 0.27 | 5.50 | 0.05 | 2.00 |
| Average for Bridge Creek Mbr. | | 1.80 | 10.35 | 0.17 | 0.57 |

*1. Table shows interpolated ages of biozone boundaries from Kauffman et al. 1993 time scale. A weighted average value for S is calculated using the base of the Bridge Creek Limestone and the top of the M. nodosoides biozone (note dashed lines) as datums.*

"raw" geochemical data to obtain the necessary regularity for spectral analysis.

To complement the geochemical data set, black and white photographs of the slabbed archive half of the Portland core were scanned to create 8-bit TIFF files and analyzed for variations in gray-scale values using Image 1.49, a public domain image analysis software package produced by the National Institutes of Health. Such programs allow for scans of optical density in which pixel gray-scale values ranging from 0 (white) to 255 (black), are averaged over a user-selected area. To produce a pixel data set as closely comparable to the geochemical data as possible, 1-2 cm areas were scanned at 5-cm intervals that corresponded to the geochemical samples. Several scans of each sample site were averaged, edited to remove spurious values (dark cracks, bright reflections, etc.), and spliced into a data series for spectral analysis (Fig. 2). As with the geochemical data, a cubic spline was applied to ensure regular spacing of data points, and values representing altered volcanic ash (bentonite) beds were edited out prior to spectral analysis.

### *Paleoecologic Data*

In collaboration with the description and geochemical sampling of the Portland core, C. Savrda analyzed trace fossil content at 2-cm intervals through the Bridge Creek Limestone (for methods see Savrda, this volume). Data for maximum burrow diameter (MBD) and oxygen-related ichnocoenoses (ORI) were chosen for spectral analysis. These represent ordinal and rank data series, respectively, and show very similar trends because ORI is partly based on MBD. For simplicity, only the ORI rank data are plotted in Figure 3.

Burns and Bralower (this volume) analyzed abundance trends of major nannofossil taxa through the bedding couplets of the Bridge Creek in the Portland core. The resulting relative abundance data (% of assemblage) are based on counts of 220 specimens in smear slides made from the same samples used in $CaCO_3$ and OC determinations (Burns and Bralower, this volume). In their study, Burns and Bralower analyzed abundant taxa at the species level, but grouped less common species by genera, assuming similar paleoecological affinities. Four taxonomic groups that fluctuate between limestone and shale hemicycles were chosen for spectral analysis. These include two groups commonly interpreted to indicate fertility (*Biscutum constans, Zygodiscus* spp.) and two groups whose paleoecological affinities are less certain (*Eiffellithus* spp., *Tranolithus* spp.) (Burns and Bralower, this volume). Because nannofossil recovery was incomplete in some samples, gaps of up to 10 or 15 cm occur in a few segments of the data series. A smoothed cubic spline was applied to interpolate between existing data points.

### *Spectral Analysis*

The fundamental challenge in spectral determination of Milankovitch forcing from geological data stems from uncertainties in age-depth relationships. These result from time-scale uncertainties, sampling problems, interference by nonperiodic climatic or geologic factors, and nonlinearity in the sedimentary expression of periodic forcing (Park and Herbert, 1987). Given these difficulties, the most reliable test for Milankovitch forcing in pre-Pleistocene geological time series is the detection of sinusoids with ratios approximating the modern orbital periods (or periods corrected to pre-Pleistocene values: Berger et al., 1989, 1992) (Park and Herbert, 1987).

In analyzing the Bridge Creek data sets we employed the multitaper method (MTM) of Thomson (1982), which is believed to provide the optimal spectral estimate in noisy geologic time series (Park and Herbert, 1987). In addition to the familiar amplitude spectra, MTM also provides a statistical test (F variance-ratio test) of the likelihood that the data contain a monochromatic signal at each discrete frequency. In our illustrations, the F-test results are superimposed on the amplitude spectra and the 90, 95, and 99% confidence levels for the F-tests are shown. All data tables include only those frequencies with F-tests above the 90% confidence level. MTM was used to test for dominant periods matching those most commonly reported in studies of Cretaceous rhythmic bedding (e.g., Fischer et al., 1985), including

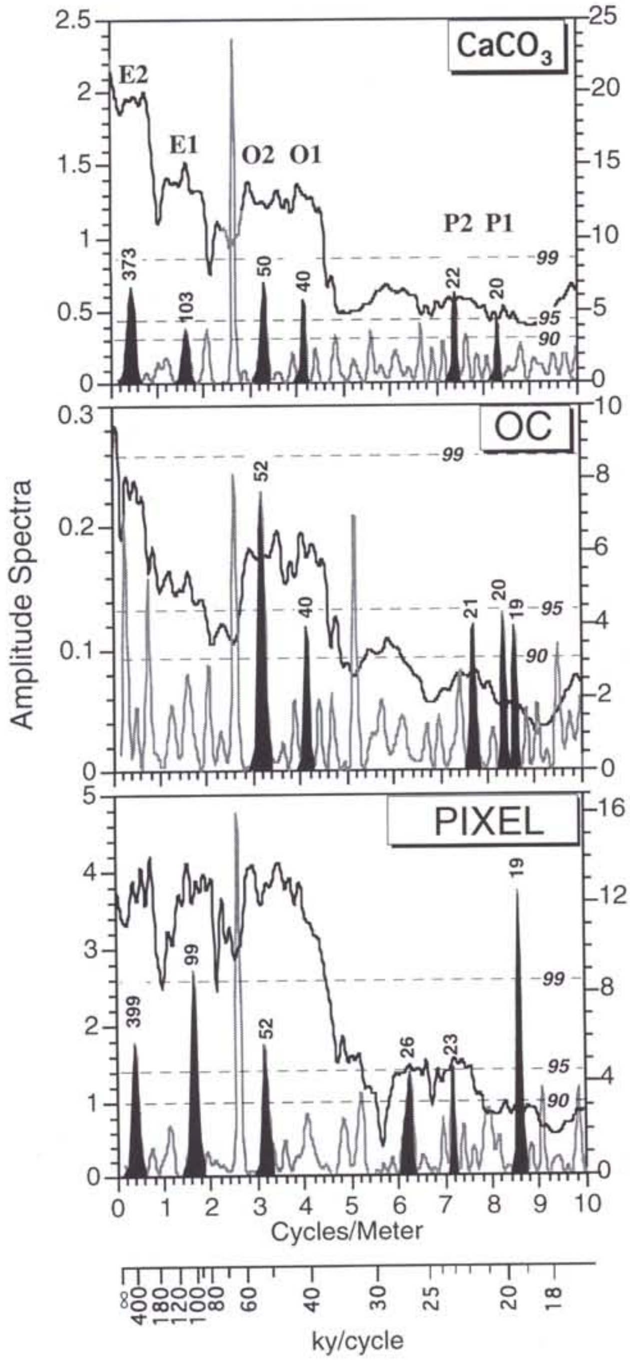


FIG. 4. Plots of multitaper method (MTM) spectra for % $CaCO_3$, % OC, and gray-scale pixel data from the upper Bridge Creek Limestone. F-test peaks (gray lines) are superimposed on amplitude spectra (black lines). The amplitude scales are on the left, the F-test scales on the right. The 90%, 95%, and 99% confidence limits for F-tests are indicated by dashed lines in each plot; they correspond to values of 3.11, 4.46, and 8.65, respectively. The blackened F-test peaks represent frequencies with F-test values >90% confidence that correspond to amplitude maxima; bold numbers show cycle periods assuming S=0.6 cm/ky (note ky/cycle scale below figure).

the 21-ky peak for precession, the 41-ky peak for obliquity, and the 100- and 413-ky peaks for eccentricity (E1 and E2). In addition, because the MTM is successful in resolving additional components of the orbital quasi-periods (Berger, 1984; Park and Herbert, 1987), we were alert to the presence of 97- and 127-ky eccentricity signals (E1a and E1b), 39 and 53 ky obliquity signals (O1 and O2), and 19- and 23-ky precession signals (P1 and P2).

Methodological steps used in the spectral analysis are described in detail in another paper (Sageman et al., 1997) and will be only briefly reviewed. The major tasks included determining appropriate MTM parameters and a reasonable age-depth relationship. MTM parameters were optimized by analyzing synthetic time series of the modern orbital parameters (Berger, 1978) constructed to parallel the Bridge Creek data sets in terms of series length. The best results were obtained with five 3-pi prolate tapers and maximum data series padding. All subsequent MTM estimates used these parameters.

Determining an appropriate age-depth relationship for the core was facilitated by new high-precision $^{40}Ar/^{39}Ar$ dates from volcanic ash beds analyzed within the study interval (Obradovich, 1993), which were used to develop an interpolated time scale for Cenomanian-Turonian biozone boundaries (Kauffman et al., 1993) (Fig. 2). Because of the scale on which sedimentation rates change in the Greenhorn Formation, and the positions of dated bentonites relative to these changes, biozone interpolation offered a better approach than a linear fit between dated horizons and stratigraphy. Based on the interpolated time scale the entire study interval represents about 1.9 Ma. Effective sedimentation rates (S), which are not corrected for compaction (Park and Herbert, 1987), can be calculated for each biozone (Table 1). An average S value of 0.57 cm/ky is determined for the study interval that contains bedding cycles, and this value is rounded to 0.6 cm/ky for analysis of the spectral results. At this rate, one meter of section represents an average time interval of 167 ky.

## RESULTS

### *Lithologic/Geochemical Data*

The lithologic characteristics of the limestone-marlstone bedding couplets in the Bridge Creek were described in detail by Pratt (1984), Arthur et al. (1985), Elder (1985), Ricken (1994), Savrda and Bottjer (1994), Sageman et al. (1997), and many others. We will first summarize those characteristics that helped guide the application of spectral methods.

The major lithotypes include a series of light-colored (light gray to medium-gray), carbonate-rich rocks such as limestone, marly limestone, and burrowed marlstones ($CaCO_3$ from >60%) and a series of dark-colored (medium light-gray or olive-gray to olive-black) marlstones and calcareous mudstones ($CaCO_3$ <60%). Fluctuations in carbonate content appear to be a dominant variable and account for the conspicuous weathering profile in outcrop as well as the light-dark color variations obvious in the core. A concomitant (but inverse) fluctuation in % OC usually occurs in the bedding couplets and may contribute to the color variation. Variations in clay content and mixing across bed boundaries due to burrowing can also influence color patterns. The idealized bedding couplet grades from a dark-colored, OC-rich, laminated marlstone upward into a light-colored, carbonate-rich, OC-poor, burrowed limestone.

Detailed plots of lithologies and variations in $CaCO_3$ and OC contents for the Bridge Creek are shown in Figure 2. Couplets in the lower half (below 600 cm in Fig. 2) generally consist of dark-colored calcareous shale or mudstone overlain by lighter-colored marlstone, marly limestone, or micritic limestone. The clay-rich hemicycles of the lower interval are anomalously low in % OC, with the exception of beds that bracket the Cenomanian-Turonian boundary, and there are numerous conspicuous bento-

TABLE 2.- *Results from MTM analysis of upper Bridge Creek Limestone.*

| Frequency (cycle/m) | Amplitude (wt.%, pix) | Phase (degrees) | F-test (>90% only) | Period-kyr (0.6cm/kyr) | |
|---|---|---|---|---|---|
| Weight %$CaCO_3$ | | | | | |
| 0.4468 | 0.0287 | 36.91 | 6.7 | **373.04** | *E2* |
| 1.6235 | 0.0197 | -110.17 | 3.88 | **102.66** | *E1* |
| 2.085 | 0.013 | 64.04 | 3.88 | 79.94 | |
| 2.6465 | 0.0167 | 69.86 | 24.52 | 62.98 | |
| 3.3081 | 0.0183 | 157.36 | 7.11 | **50.38** | *O2* |
| 4.1602 | 0.0185 | 62.48 | 5.81 | **40.06** | *O1* |
| 4.8462 | 0.0077 | 175.2 | 3.4 | 34.39 | |
| 5.5957 | 0.007 | -82.45 | 3.63 | 29.78 | |
| 6.6724 | 0.0063 | 19.59 | 4.16 | 24.98 | |
| 7.4097 | 0.0083 | 42.55 | 6.47 | **22.49** | *P2* |
| 7.644 | 0.0073 | -65.02 | 3.43 | 21.8 | |
| 8.3203 | 0.0064 | 42.63 | 4.3 | **20.03** | *P1* |
| Weight %OC | | | | | |
| 0.2759 | 0.0034 | 135.72 | 7.1 | 604.13 | |
| 0.7666 | 0.0024 | -41.9 | 5.43 | 217.41 | |
| 2.6172 | 0.0016 | -67.62 | 8.15 | 63.68 | |
| 3.208 | 0.0026 | 59.14 | 7.77 | **51.95** | *O2* |
| 4.1577 | 0.0023 | -126.84 | 3.96 | **40.09** | *O1* |
| 5.1831 | 0.0011 | -13.52 | 7.21 | 32.16 | |
| 7.7075 | 0.0011 | 45.77 | 4 | **21.62** | *P2* |
| 8.3569 | 0.0007 | 172.75 | 4.3 | 19.94 | |
| 8.5962 | 0.0006 | 31.55 | 3.97 | **19.39** | *P1* |
| 9.5044 | 0.0007 | 61.79 | 3.47 | 17.54 | |
| Grayscale Pixel Value | | | | | |
| 0.4175 | 0.0544 | -73.94 | 5.75 | **399.22** | *E2* |
| 1.6773 | 0.0561 | 39.84 | 8.69 | **99.37** | *E1* |
| 2.6221 | 0.0495 | -138.14 | 15.54 | 63.56 | |
| 3.1812 | 0.0528 | 53.26 | 5.63 | **52.39** | *O2* |
| 5.2368 | 0.02 | -113.28 | 3.59 | 31.83 | |
| 6.2842 | 0.02 | 5.48 | 4.57 | 26.52 | |
| 7.1997 | 0.022 | -167.85 | 4.62 | **23.15** | *P2* |
| 8.6206 | 0.0134 | -21.09 | 12.71 | **19.33** | *P1* |
| 9.0942 | 0.0089 | 30.05 | 3.73 | 18.33 | |
| 9.8706 | 0.011 | 105.54 | 3.86 | 16.88 | |

*1. Only frequencies with F-tests above 90% confidence level are shown.*

*2. Frequency values close to the dominant orbital cycles are designated as E1, E2, etc. on the right, and their period values are printed in bold.*

nites. In addition, some limestone beds are anomalously thick; based on regional stratigraphic data these beds were interpreted to represent amalgamation of several thinner limestones (Sageman et al., 1997). In contrast, most of the bedding couplets in the upper Bridge Creek Member (above 600 cm in Fig. 2) consist of dark-colored marlstone overlain by light-colored marly or micritic limestone and show an overall increase in $CaCO_3$ and OC content. Bioturbation trends closely follow the lithologic oscillations (Fig. 3), and there is a decrease in bed thicknesses and a shift to more regular oscillations between the two end-member depositional phases of the upper Bridge Creek. In fact, the hemicycles show a coordinated (but inverse) oscillation in $CaCO_3$ and OC content at both shorter (bedding cycles) and longer (meter-scale) wavelengths (Fig. 2). These data suggest that a major change occurred in the nature of deposition from the lower part to the upper part of the Bridge Creek Limestone. A quantifiable record of orbital influence on the depositional system, if it is preserved at all, should be most clearly recorded in the upper part of the study interval. Spectral analyses supported this conclusion, and thus all spectral results reported herein are limited to the data series from 600 to 1230 cm, which represents about 0.8 - 0.9 Ma (Fig. 2).

The results of MTM analysis of the % $CaCO_3$, % OC and gray-scale pixel data from the upper part of the Bridge Creek are

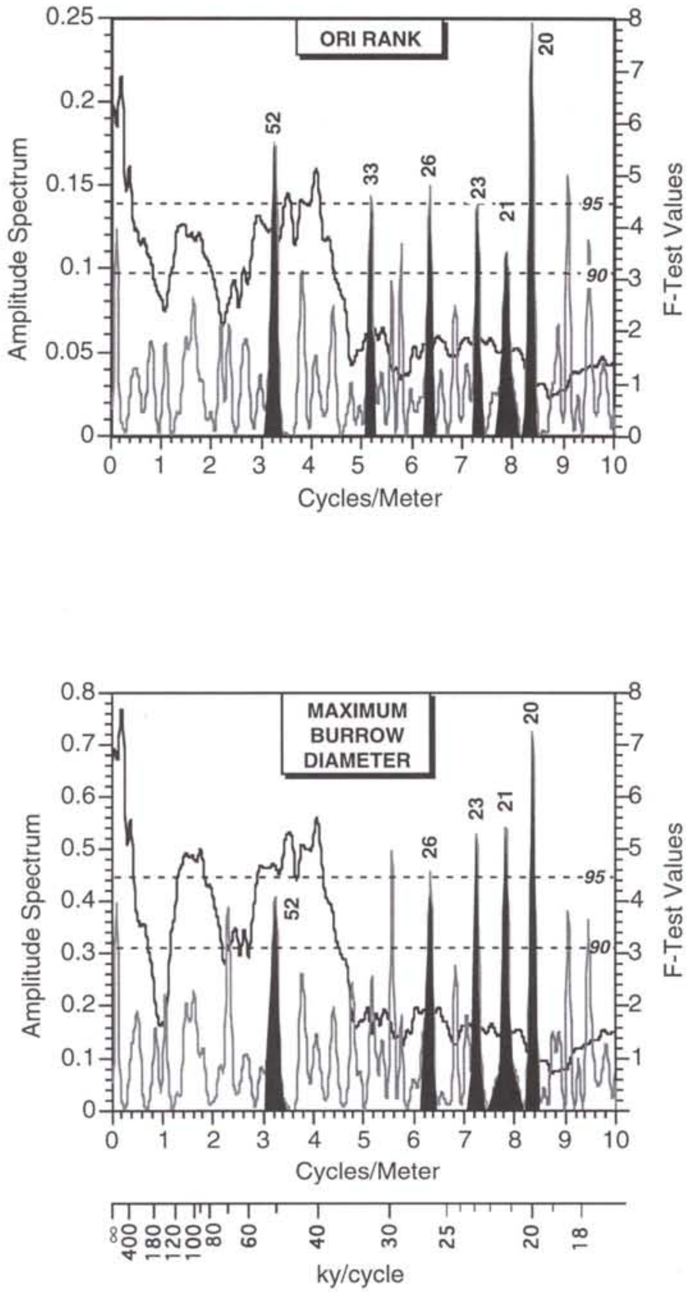


FIG. 5. Plots of multitaper method (MTM) spectra for oxygen-related ichnocoenosis rank (ORI) and maximum burrow diameter (MBD) from the upper Bridge Creek Limestone. F-test peaks (gray lines) are superimposed on amplitude spectra (black lines). The blackened F-test peaks represent frequencies with F-test values >90% confidence that correspond to amplitude maxima; bold numbers show cycle periods assuming S=0.6 cm/ky (note ky/cycle scale below figure).

shown in Figure 4 and tabulated in Table 1. The F-test output indicates scattered noise below the 90% confidence level, but also shows a series of peaks with F-tests >90% within the ranges of about 0.4, 1.6, 3.3, 4.1, and 7.0-8.5 cycles/m (darkened in Fig. 4). At a sedimentation rate of 0.6 cm/ky, which was estimated for the upper Bridge Creek Member based on the interpolated biozone boundary ages, these peaks correspond closely to the frequencies for the E2, E1, O2, O1, and P2-P1 orbital cycles, respectively (Table 2). Variations in the spectral results among the different data sets are summarized as follows:

1. % $CaCO_3$ shows distinct plateaus in the amplitude spectrum corresponding to E and O signals, and a weaker and broader plateau at frequencies corresponding to P. However, significant F-test results occur for E1, E2, O1, O2, and P1 - P2. All but one of these F-test peaks is above the 95% confidence level.
2. % OC shows a dominant plateau in the amplitude spectrum that corresponds to the obliquity signal. F-test results confirm this with significant peaks for O1 and O2. The O2 peak is above the 95% confidence level. Several peaks with F-tests above the 90% confidence level also occurred at frequencies suggesting that there might be a precessional signal.
3. Gray-scale pixel data show strong amplitude plateaus at frequencies corresponding to E and O, and significant F-test responses for E1, E2, O2, and P1/P2. The F-test peaks for E1 and P1 were above the 99% confidence level and strongly suggest the precessional index.
4. Peaks with F-tests >90% confidence that do not match the dominant Milankovitch periods were also observed at 2.6 cycles/m in all three data sets and at 5.2 cycles/m in % OC. Note that these peaks correlate with troughs in the amplitude spectrum; as such they only indicate a well-defined lack of strength in the signal at that frequency.

In summary, spectral analysis of the lithologic/geochemical data suggest that there is evidence for each of the major orbital parameters. The amplitude records show conspicuous plateaus at 3-4 cycles/m corresponding to the obliquity cycle, and significant F-tests appear for O1 and O2 in spectra for % $CaCO_3$ and % OC. Interestingly, O2 produces a stronger signal, which is especially pronounced in the % OC data. Although a number of F-tests with >90% confidence could be produced purely by chance, the likelihood that they would conform so closely to the ratio of the Cretaceous orbital periods (Table 3) is extremely small. One possible explanation for anomalous peaks in the F-test record is the influence of halftones or overtones. For example, the normally weak 52-ky peak may have been amplified in the record by the beat frequency of another quasiperiod.

### *Ichnologic Data*

Systematic variations in the diversity, diameter, and penetration depth of burrows are common features of limestone-marlstone cycles in pelagic and hemipelagic strata (Savrda and Bottjer, 1994). In the Bridge Creek Limestone, for example, a change from laminated, organic carbon-rich shale (OC>6%) to densely burrowed limestone (OC<1%) is typical of many bedding couplets. Savrda and Bottjer (1994) analyzed these variations in the lower part of the study interval using acetate peels of a core drilled at Rock Canyon Anticline near Pueblo, Colorado (Pratt, 1984). They identified four recurrent ichnocoenoses defined by their trace fossil assemblages: (1) *Chondrites* ichnocoenosis; (2) *Planolites* ichnocoenosis; (3) *Zoophycos/Teichichnus* ichnocoenosis; and (4) *Thalassinoides* ichnocoenosis. Using measurements of trace fossil diversity, maximum burrow diameter, penetration depth, and vertical stacking patterns, Savrda and Bottjer (1994) interpreted a history of changes in benthic paleo-oxygenation that correspond to the lithologic changes of the bedding couplets. Savrda (this volume) employed the same techniques to analyze the Bridge Creek study interval in the Portland core, and Figure 3 includes a plot of oxygen-related ichnocoenosis (ORI) rank values from his study.

Several features of the ORI plot are relevant to our investi-

TABLE 3.- *Analysis of MTM frequency data.*

| | E2 | E1 | O2 | O1 | P2 | P1 |
|---|---|---|---|---|---|---|
| $CaCO_3$ | >95 | >90 | >95 | >95 | >95 | >90 |
| OC | - | (<90) | >95 | >90 | >90 | >90 |
| Pixel | >95 | >99 | >95 | (<90) | >90 | >99 |
| f (cycles/m) | 0.432 | 1.65 | 3.23 | 4.16 | 7.44 | 8.51 |
| $\sigma$ (cycles/m) | 0.02 | 0.04 | 0.07 | 0.002 | 0.26 | 0.17 |
| Period (kyr) | 385.8 | 101 | 51.6 | 40.06 | 22.4 | 19.58 |
| Scaled ratio | 3.79 | 0.99 | 0.507 | 0.39 | 0.22 | 0.19 |
| Predicted ratio | 4.09 | 1 | 0.507 | 0.388 | 0.229 | 0.185 |

1. *Only spectral peaks with at least two F-test values >90% confidence among the three data series ($CaCO_3$, OC, and gray-scale) were used.*

2. *F-test confidence levels for the peaks corresponding approximately to frequencies for E2, E1, O2, O1, P2, and P1 are shown at top for $CaCO_3$, OC and Pixel data sets. Calculated values include: average of the frequency (f), standard deviation ($\sigma$) , the corresponding period using a sedimentation rate of 0.6 cm/kyr, and the ratio between the resulting periods. The ratio is calculated by setting peaks with the strongest response (e.g., O2 > 95% confidence in all three data sets) to 0.507, which is equivalent to its estimated Cretaceous value, and scaling the other values accordingly. Based on the standard deviations shown, the error in period estimates among the different data records is E2±18.7 kyr; E1±2.38 kyr; O2±1.09 kyr; O1±0.02 kyr; P2±0.75 kyr; and P1±0.38 kyr. Finally, the scaled ratio is compared to that predicted for Cretaceous orbital cycles by Berger et al. (1989).*

gation. For example, burrowing intensity appears to correlate positively with the thickness and carbonate content of limestone beds. Thicker beds are characterized by ORI Rank 4. The thinner limestone or marlstone beds between them show lower rank values, and these are interbedded with laminated units (Fig. 3). In the lower part of the Bridge Creek Limestone, Savrda and Bottjer (1994) identified bundling in these burrowing trends that suggests the precessional index. Analysis of the Portland core (Savrda, this volume) showed that the same bundling does not occur in the upper part of the member. In fact, there is an overall decrease in burrowing levels within the clay-rich hemicycles from the lower to the upper part of the Bridge Creek, and fluctuations from laminated to highly burrowed hemicycles become much more pronounced (Fig. 3).

The multitaper method was applied to the data series for maximum burrow diameter (MBD) and ORI rank from the upper Bridge Creek Limestone. The analysis parameters were the same as those used for the lithologic and geochemical data sets. The results of the analyses were nearly identical for both types of ichnological measurements, which is to be expected given that the two measures represent strongly correlated dependent variables (Savrda and Bottjer, 1994). Results of MTM analyses are summarized in Figure 5 and Table 4.

The amplitude curves in Figure 5 show pronounced plateaus at 1.6 and 3-4 cycles/m. F-test results do not support the 1.6 cycle/m peak but include a >95% confidence peak at 3.3 cycles/m. In addition, multiple peaks above the 95% confidence level occur in the 7-8.5 cycles/m range. Using S = 0.6 cm/ky, these results correspond to O2 and P1/2 periodicities. Peaks below the 90% limit for E1 and O1 that correlate to significant signals in the lithologic/geochemical data were also observed but are statistically indistinguishable from signal noise.

Given our estimated sedimentation rate, the strongest signals in the ichnologic data correlate with frequencies suggesting obliquity and precession. The similarity between amplitude spectra for MBD and ORI Rank and those for $CaCO_3$, OC, and pixel values suggests that variations in bottom-water oxygenation (MBD and ORI), clastic influx ($CaCO_3$ dilution), and preservation of organic matter are linked and are collectively driven by orbital forcing. The ichnologic spectra are most similar to spectra for % OC.

### *Nannofossil Data*

A detailed analysis of relative abundance trends in nannofossils through the entire sequence of bedding couplets in the Bridge Creek Limestone was conducted on the Portland core by Burns and Bralower (this volume). Although a large number of nannofossil taxa were counted, Burns and Bralower (this volume) focus on seven species or species groups that comprise the bulk of species abundance in the assemblages. Several of these taxa have been widely used for interpretations of taphonomy and paleoenvironmental conditions (Burns and Bralower, this volume). For example, the abundance of *Watznaueria barnesae,* a solution-resistant taxon, suggests that nannofossil preservation in the Portland core is comparatively poor. A decrease in abundance of *W. barnesae* and an increase in nannofossil species richness (Burn and Bralower, this volume) in the upper Bridge Creek Member, however, suggests preservation is better there and that valid paleoecological interpretations might be made for this part of the study interval. Thus, a decision to focus spectral analysis on the upper interval for comparative purposes is supported by preservational arguments as well.

Species or species groups commonly interpreted as fertility indicators include *Biscutum constans* and *Zygodiscus* spp. (e.g., Roth and Bowdler, 1981; Roth and Krumbach, 1988; Watkins,

TABLE 4.- *MTM analysis of ichnologic data from upper Bridge Creek Limestone.*

| Frequency (cycles/m) | Amplitude (MBD/ORI) | Phase (degrees) | F-test (>90% only) | Period-kyr (0.6cm/kyr) | |
|---|---|---|---|---|---|
| Maximum Burrow Diameter | | | | | |
| 0.1038 | 0.0029 | -55.21 | 3.96 | 1606.27 | |
| 2.3193 | 0.0013 | 17.27 | 3.88 | 71.86 | |
| 3.2532 | 0.002 | 65.45 | 4.07 | **51.23** | *O2* |
| 5.5847 | 0.0007 | 94.68 | 4.95 | 29.84 | |
| 6.3477 | 0.0009 | -87.24 | 4.57 | 26.26 | |
| 7.2693 | 0.0007 | -136.24 | 5.29 | **22.93** | *P2* |
| 7.8491 | 0.0007 | -160.94 | 5.42 | 21.23 | |
| 8.3801 | 0.0005 | -71.17 | 7.22 | **19.89** | *P1* |
| 9.0759 | 0.0004 | -26.98 | 3.79 | 18.36 | |
| 9.4727 | 0.0005 | -173.72 | 3.64 | 17.59 | |
| ORI Rank | | | | | |
| 0.1038 | 0.0008 | -61.38 | 3.98 | 1606.27 | |
| 3.2532 | 0.0006 | 62.82 | 5.54 | **51.23** | *O2* |
| 3.7903 | 0.0006 | -35.69 | 3.17 | **43.97** | *O1* |
| 5.1636 | 0.0002 | -152.75 | 4.61 | 32.28 | |
| 5.7678 | 0.0002 | 55.13 | 3.7 | 28.9 | |
| 6.3416 | 0.0002 | -71.12 | 4.83 | 26.28 | |
| 7.2815 | 0.0002 | -154.01 | 4.45 | **22.89** | *P2* |
| 7.8613 | 0.0002 | -167.84 | 3.53 | **21.2** | |
| 8.3557 | 0.0002 | -47.31 | 7.91 | **19.95** | *P1* |
| 9.0759 | 0.0001 | -19.94 | 5.01 | 18.36 | |
| 9.491 | 0.0002 | 173.23 | 3.76 | 17.56 | |

*1. Only frequencies with F-tests above the 90% confidence level are shown.*

*2. Period values were calculated using S = 0.6 cm/kyr. Frequency values close to the dominant orbital cycles are designated as E1, E2, etc. on the right, and their period values are printed in bold.*

1989; Erba et al., 1992). Watkins (1989) observed that these taxa were relatively abundant in OC-rich or clay-rich hemicycles and less abundant in carbonate-rich beds. Although this relationship holds for many of the hemicycles in the Portland core, it is not entirely consistent from one hemicycle to the next, and the two taxa do not always covary closely (Fig. 3). A 5-point moving average curve through the data for *B. constans* and *Zygodiscus* spp. also does not indicate a common trend. In fact, whereas *Zygodiscus* spp. is most abundant in the lower part of the study interval, *B. constans* is least abundant there and reaches a maximum in the upper interval (Fig. 3). Nonetheless, because these taxa are established fertility proxies, they were analyzed with MTM. Two other taxa, *Eiffellithus* spp. and *Tranolithus* spp., were also chosen for analysis from among those studied by Burns and Bralower (this volume). Although Watkins (1989) correlated *Eiffellithus* spp. with limestone deposition and suggested that it reflected low fertility levels, Burns and Bralower (this volume) found no significant correlation between *Eiffellithus* spp. and $CaCO_3$ content. However, *Eiffellithus* spp. and *Tranolithus* spp. show a range of behaviors in terms of fluctuations between limestone and shale hemicycles as well as some longer-term fluctuations in relative abundance (Fig. 3) and thus were considered appropriate for spectral analysis.

As in prior MTM analyses, only nannofossil data points above 600 cm (Fig. 3) were analyzed. This limits the effect of changes in nannofossil populations associated with OAE II (Schlanger et al., 1987) and the Cenomanian-Turonian extinction event, and focuses on the best preserved assemblages. Identical MTM parameters were used for the nannofossil analyses as employed in analyses of previous data sets. Like the results for MBD and ORI Rank, output from the nannofossil analyses includes various F-test peaks above the 90% confidence level (Fig. 6). Although some of these peaks match lows in the amplitude spectrum (e.g., peaks at 2.6 and 4.8 cycles/m in the *B. constans* plot), others do not. These may reflect either beat frequencies as suggested earlier, complicated and/or noisy signals, or nonlinear effects in the spectrum.

Distinct amplitude plateaus occur in the *B. constans* output from 1.5 to 1.8 cycles/m and from 3.0 to 4.6 cycles/m (Fig. 6). Although less pronounced than the amplitude plateaus of lithologic and ichnologic data sets, they are similar in frequency range. The *B. constans* F-test output is also similar to previous spectral estimates. It shows peaks above 95% confidence at 1.8, 3.4, and 6.8 cycles/m, which suggests frequencies within the range of E1, O2, and P2, respectively. Although some peaks are above the 90% confidence level, as would be predicted, those that correlate to orbital frequencies are the most significant. Among the nannofossil data tested, *B. constans* is the only taxon that produced spectra reasonably similar to those previously discussed.

The results for *Zygodiscus* spp. include several significant

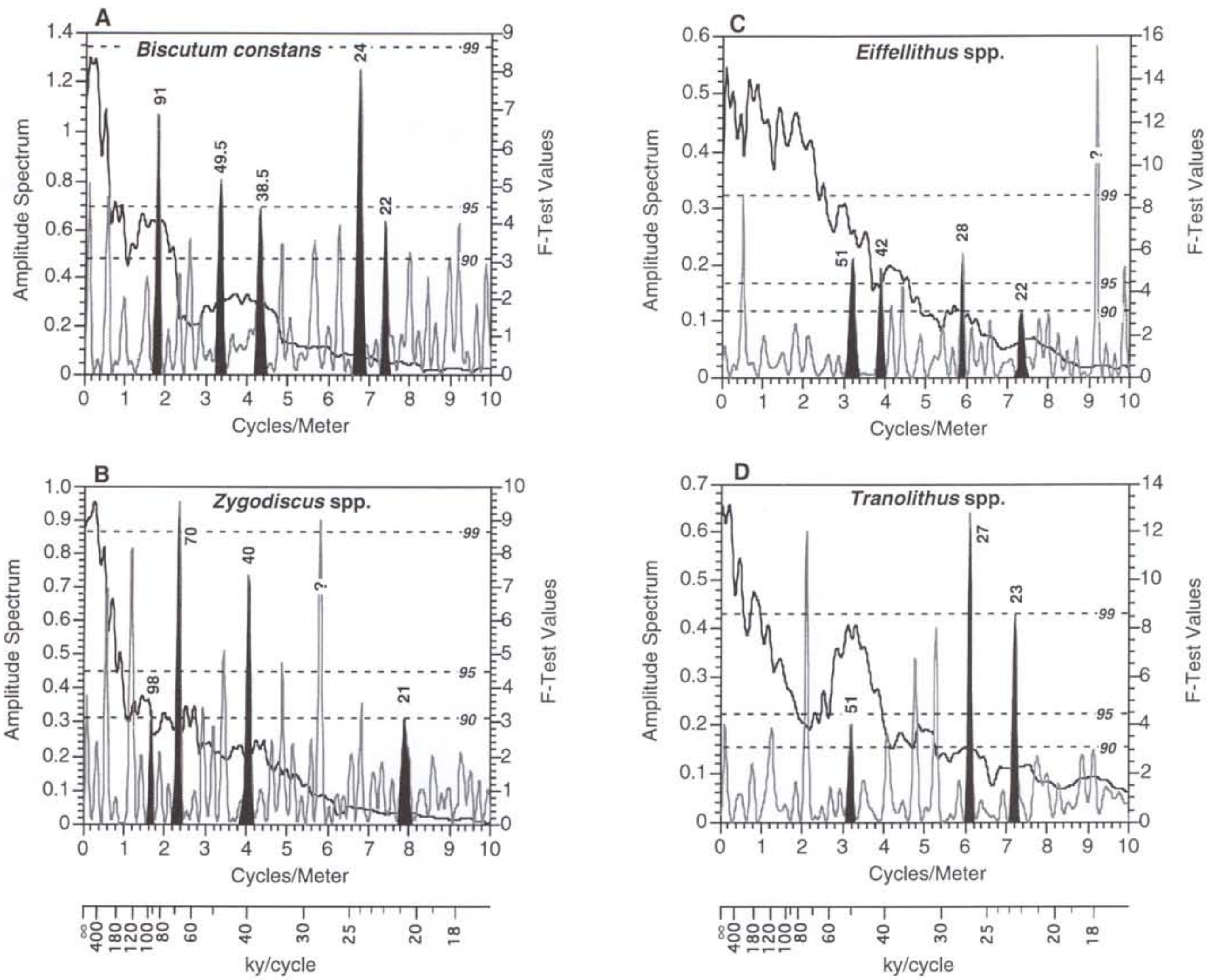


FIG. 6. Plots of multitaper method (MTM) spectra for (A) *B. constans*, (B) *Zygodiscus* spp., (C) *Eiffellithus* spp., and (D) *Tranolithus* spp. from the upper Bridge Creek Limestone. F-test peaks (gray lines) are superimposed on amplitude spectra (black lines). The blackened F-test peaks represent frequencies with F-test values >90% confidence that correspond to amplitude maxima; bold numbers show cycle periods assuming S=0.6 cm/ky (note ky/cycle scales below plots).

F-test peaks, but the amplitude record shows very weak response above a red noise spectrum. Thus, although certain peaks suggest the E1, O1, and P1 signals (at 1.7, 4.0, and 7.9 cycles/m, respectively), there are several other highly significant F-tests for frequencies that do not match orbital signals or reflect low points in the amplitude spectrum. These results suggest that there is considerable noise in the record and fail to clearly support an hypothesis of orbital influence. Although the *Eiffellithus* spp. results are similarly inconclusive, the amplitude spectrum for *Tranolithus* spp. reflects a possible O2 signal (note F-test >90% confidence for 51 ky), as well as a possible P2 signal (note F-test >99% confidence for 23 ky). The peak at 27 ky (F-test >99% confidence) has a corresponding amplitude response and while it is not correlated to an orbital quasi-period, may represent an interference tone.

## DISCUSSION

Using sedimentologic, paleontologic, and geochemical evidence, many authors (e.g., Arthur et al., 1984, 1985; Barron et al., 1985; Pratt et al., 1993) have argued for a coordinated dilution-redox mechanism to explain the development of the Bridge Creek bedding couplets. In this model, increased rainfall in the highlands to the west increases freshwater input to the seaway which, in turn, increases the delivery of fine-grained siliciclastics throughout the basin (causing dilution of the carbonate flux to the sediment) and stratification of the water column (leading to lower benthic oxygen levels and increased OC preservation). The result is deposition of laminated, OC-rich shale or marlstone. Alternately, drier periods of low fresh-water input are characterized by decreased supply of fine-grained sediment, a clearer, better-mixed water column, increase in benthic oxygen levels, possible improvement in conditions for calcareous phytoplankton production, and deposition of a burrowed limestone. The driving force in this model is the modulation of climate by orbital influences to produce variations in precipitation over the land areas draining into the basin.

Other authors have argued that the planktonic microfossil record of the Western Interior basin does not support the interpretation of "freshened" surface waters during deposition of clay-

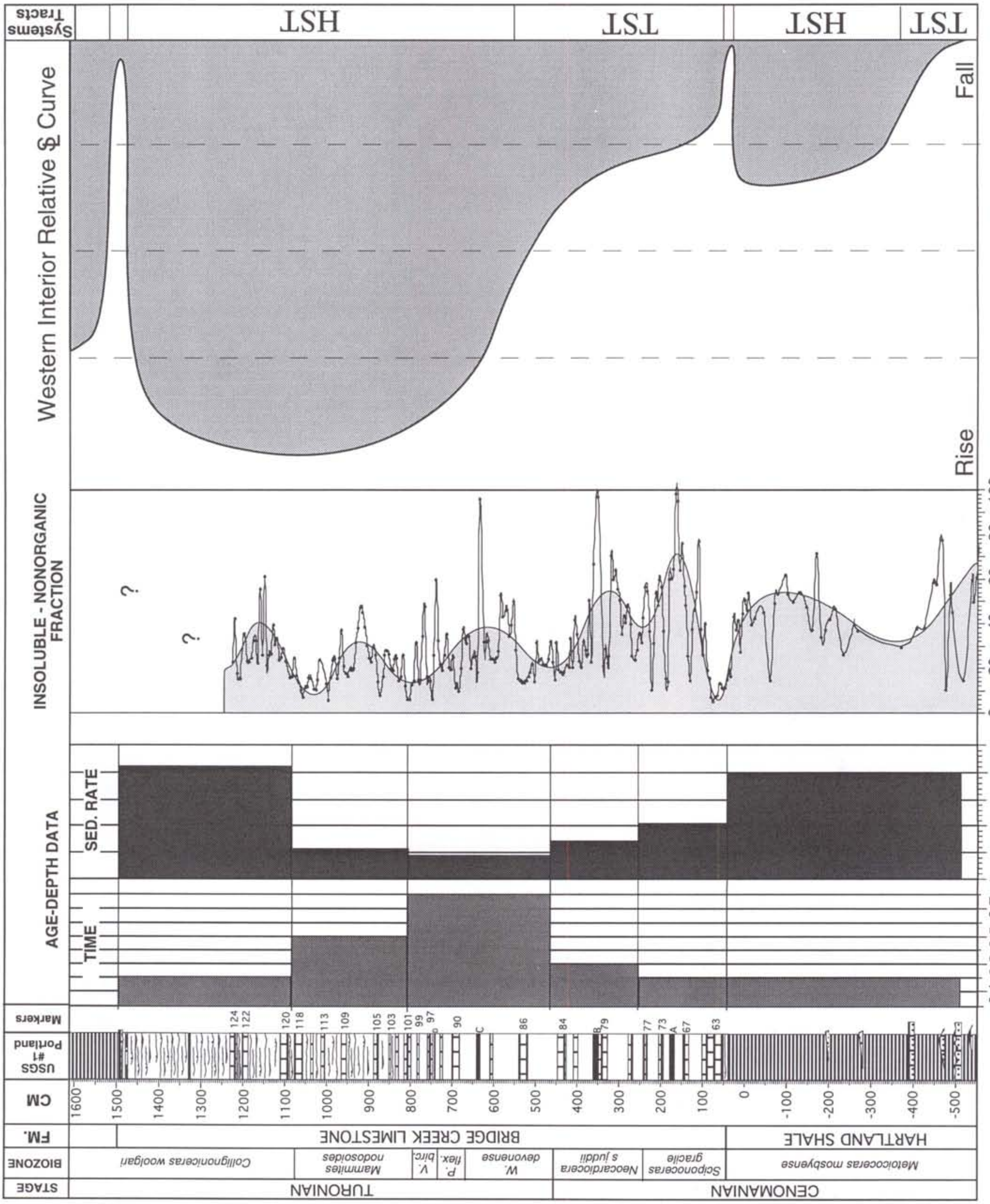


FIG. 7. Measured section of the Portland core with histograms showing duration of selected biozones and corresponding sedimentation rates, a plot of weight % insoluble-nonorganic fraction (INF) with superimposed 20-point moving average (MA) curve (see text), and an interpretation of relative sea level change based on regional stratigraphy and facies analysis (modified from Sageman, 1996). Equivalent systems tract designations (sensu Haq et al., 1987) are also shown.

rich hemicycles and suggest instead that changes in oceanic primary productivity due to cycles of nutrient upwelling could account for the bedding couplets (Eicher and Diner, 1985, 1989). In this model, orbital forcing leads to changes in evaporation at low latitudes sufficient to cause warm, saline bottom waters to form, which in turn displace nutrient-rich oceanic deep waters to the surface. Nutrient-driven blooms of phytoplankton would occur along the northern margin of the Tethys Sea and would have influenced the Western Interior basin through its southern aperture. A problem for this model, however, is suggested by the results of Watkins (1989) which indicate that high productivity characterizes the clay-rich (OC-rich) hemicycles rather than the carbonate-rich phases. Watkins (1989) suggests that the cycles do indeed reflect dilution, but in this case, dilution of the carbonate flux by organic matter.

Arthur and Dean (1991) and Ricken (1991 and 1994) argued that patterns in bedding cycles may be understood in terms of the mixing of three primary fluxes, detrital clay, $CaCO_3$ and OC, as well as the degree of subsequent modification due to carbonate dissolution, OC oxidation from biogenic activity, and other diagenetic factors. Analyzing elemental, organic, and isotopic geochemical data, Arthur and Dean (1991) concluded that the Bridge Creek bedding couplets were dominantly controlled by dilution of carbonate through orbitally forced changes in the detrital flux, but that changes in the productivity of calcareous plankton probably also played an important but secondary role. Arthur and Dean (1991) pointed out the need to understand the nature of the different fluxes to the sediment as well as the degree to which they represent dependent or independent variables. For example, the observed correlation between aluminum and OC in the Bridge Creek Member was interpreted to reflect a linkage of independent variables by a common forcing factor (higher freshwater input causes increase in detrital flux as well as enhanced water-column stratification leading to better preservation of OC), rather than a direct relationship (OC is adsorbed on clays, thus higher detrital flux leads to enhanced OC burial). However, because OC content in marine strata is ultimately controlled by a combination of organic production, bulk sedimentation rate, and redox conditions (that influence benthic biogenic activity) (Arthur and Sageman, 1994), the implications of linkage are not so clear.

Thus, the most important unanswered questions concerning Western Interior bedding cycles relate to the nature and origin of linkages: (1) Is OC production necessarily linked to carbonate production, and can changes in nannofossil and planktonic foraminiferal assemblages occur independently of changes in the noncalcareous phytoplankton and vice versa? (2) Are changes in OC and carbonate production linked to oceanic nutrient cycles, to nutrient input from fluvial sources, or to a combination of both, and do they respond independently to these forcing factors? (3) Is OC content primarily controlled by organic production, by preservation due to water column stratification and resulting oxygen deficiency, or to a combination of both? and (4) Does the influence of orbitally forced changes in climate impart an overall coordination to multiple independent processes, and, if so, how is this accomplished?

Our purpose was to first address whether or not the bedding couplets could be quantitatively related to orbital cyclicity using spectral techniques, and then to employ spectral results from independent data records as a tool to interpret links between different components of the depositional system. The bedding couplets of the Bridge Creek Limestone are complex and do not consistently show a 1:5 ratio like other Cretaceous limestone-marlstone units (Schwarzacher and Fischer, 1982). Nor do they show the uniform bedding characteristic of couplets that are interpreted to result from obliquity (Fischer at al., 1985). Comparing the spectral signatures of % OC, % $CaCO_3$, and gray-scale data with those for burrow diameter and nannofossil abundance in the Bridge Creek Member, Portland core, provides an opportunity to test the Milankovitch hypothesis more rigorously and a way to evaluate the relationships between lithology, benthic oxygen, and planktic productivity during Cenomanian-Turonian time.

### *Sources of Error*

Sources of error that could influence the interpretations described herein include variability in sedimentation rates within and between bedding couplets, time-scale errors, and errors introduced in the process of spectral analysis. For example, it is estimated that given a series of 100 data points, there may be up to 10 F-test peaks from the MTM estimate that are above the 90% confidence level completely by random chance (Thomson, 1982). However, because most of our data sets showed consistent and significant F-test responses at frequencies that closely approximate the ratio of orbital cycles (Table 3), they were judged to reflect Milankovitch cyclicity.

To objectively assess variation in sedimentation rates one must analyze time-scale errors. Although the radiometric dates used in this study are the best available for the Upper Cretaceous (Obradovich, 1993), they nonetheless have an average error of ±0.6 Ma. This means that bulk sedimentation rates could have varied by as much as 1 cm/ky from the average value used here (Table 1). Clearly this would significantly affect the interpretation of MTM spectra. However, the average sedimentation rate of 0.6 cm/ky is close to that estimated for other Cretaceous hemipelagic facies (e.g., Park and Herbert, 1987), and is within the range of bulk sedimentation rates estimated in previous studies of the Bridge Creek Limestone (Pratt, 1985).

Although the question of variations in sedimentation rate within individual bedding couplets is difficult if not impossible to resolve, Ricken's (1994) calculations of changes in relative sedimentation rate from clay-rich to carbonate-rich hemicycles of the lower Bridge Creek Member suggest that they are minor (<0.10 cm/ky). Such differences as indicated by Ricken (1994) would be least in the upper part of the study interval, where the bedding rhythms are most uniform and sedimentation rates are lowest (Fig. 7). Anomalies in trends of bed thickness, $CaCO_3$, and OC, and regional stratigraphic relationships (Sageman, 1991, Sageman et al., 1997), as well as direct calculation of age-depth relationships in the core (Fig. 7) show that sedimentation rates changed significantly from the lower to the upper part of the study interval. The change in sedimentation rate can be correlated to an increase in the weight percent of the insoluble, non-organic fraction [100-(% CaCO3 + % OC)], called the INF, and reflects increases in the contribution of detrital and/or volcanic clay to the sediment. Variations in the INF upsection are consistent with predictions based on interpretation of relative sea-level change for the Greenhorn Formation (Sageman, 1996). The lower Bridge Creek records a transgressive episode during which sediment delivery to the basin changed rapidly. Volcanic ash may have diluted detrital, carbonate, and organic fractions due to decreased background detrital sediment flux or intensified eruptive activity. The decrease in detrital clastic flux from the lower to upper Bridge Creek corresponds well with a decrease in calculated sedimentation rate, and suggests that the maximum rate of relative sea level rise occurred just after the Cenomanian-Turonian boundary event and resulted in a condensed section (sensu Van Wagoner et al., 1988) in the earliest Turonian.

*Significance of Paleoecologic Data*

Addressing the dominant influences on preserved ORI's, Savrda and Bottjer (1994) discussed a complex set of control mechanisms and feedbacks related to OC preservation. Bottom-water oxygen levels may be most strongly controlled by pore-water oxygen, which in turn is influenced by the OC content of sediments and bacterial activity (e.g., Tyson, 1987). Sediment OC content in a shallow epicontinental sea is mainly controlled by organic production, rate and mechanism of OC transport through the water column, burial rate, sediment grain size, and perhaps most important, the rate of consumption by bacteria and macrofauna in the benthic transition layer. Because biotic activity is largely controlled by $O_2$ levels, the rate of OC supply vs. the rate of oxygen advection to the benthic zone is the key factor limiting biotas, and thus organic richness of the sediment. Savrda and Bottjer (1994) noted, however, that additional factors, such as the consistency of substrates, could influence infaunas and impart some control on burrowing patterns. Based on these factors, three hypotheses may be formed: (1) if ORI's mainly depend on physical changes in the substrate due to dilution or productivity cycles, they should correlate with changes in % $CaCO_3$ (and have similar spectra); (2) if ORI's mainly depend on changes in organic richness and pore water $O_2$, they should correlate with changes in % OC (and have similar spectra); and (3) if ORI's correlate with either % $CaCO_3$ or % OC because of a common external forcing mechanism, they should have similar spectra.

Comparison of Figures 4 and 5 shows that the spectra for ORI Rank and MBD are most similar to that for OC; each indicates dominance of obliquity and precession, but there is no statistically significant record of eccentricity. This result suggests stronger coupling between bioturbation and OC content of substrates than between bioturbation and $CaCO_3$ content (and presumed substrate consistency). However, it does not resolve whether changes in OC content reflect increased OC flux or decreased $O_2$ advection. The spectral result also indicates that the records of OC and $CaCO_3$ may be decoupled, and perhaps slightly out of phase, which suggests that the mechanisms responsible for OC production or water column stratification in the basin are different from those that control carbonate production (or siliciclastic dilution).

Although nannofossil assemblages from strata of the Western Interior basin have been described as unusual and enigmatic compared to assemblages from oceanic settings, levels of diversity nonetheless reach oceanic values in the peak transgressive Bridge Creek Limestone of the Greenhorn Cyclothem (Watkins et al., 1993). Watkins (1989) analyzed nannofossil assemblages in Bridge Creek limestone/marlstone bedding couplets and found that changes in assemblage diversity correlated significantly with changes in % $CaCO_3$. Based on analysis of two couplets at localities in Kansas, Nebraska, and South Dakota, Watkins (1989) found that limestone hemicycles tend to be characterized by high diversity and high equitability levels whereas marlstone hemicycles show lower diversity and dominance of species that reflect high fertility (e.g., Roth and Krumbach, 1986). Certain species showed strong correlations in relative abundance to the carbonate-rich hemicycles (e.g., *Helicolithus* or *Eiffellithus* spp.) while others correlated significantly with the organic carbon-rich laminated marls (e.g., *Biscutum constans, Zeugrhabdotus* or *Zygodiscus* spp.).

Watkins (1989) interpreted these trends as reflective of changes in surface water conditions related to climate cycles. He suggested that the deposition of organic carbon-rich marlstone hemicycles was characterized by unstable conditions in the water column, increased nutrient levels, and high fertility among a few opportunistic taxa. Carbonate-rich hemicycles, on the other hand, were characterized by more stable conditions leading to higher diversity and equitability levels. Watkin's (1989) results contradict the suggestion of Eicher and Diner (1985 and 1989) that high productivity levels accounted for the deposition of Bridge Creek limestone beds.

Comparison of trends in the nannofossil record with % $CaCO_3$, % OC, and bioturbation offers an opportunity to assess linkages between surface-water conditions, sedimentation processes, and redox history. Burns and Bralower (this volume) indicate that several taxa have specific interpretive value: *W. barneseae* reflects nannofossil preservation and *B. constans* indicates fertility. Poor results in nannofossil spectra for the Portland core may reflect poor preservation, as suggested by trends in *W. barnesae* (Burns and Bralower, this volume), or they may indicate that changes in the relative abundance of some taxa (e.g., *Zygodiscus* spp., *Eiffellithus* spp.) are unrelated to the forcing factors that influence the depositional system. The spectrum for *B. constans*, however, showed a result most similar to that for % $CaCO_3$, and the spectrum for *Tranolithus* spp. was similar to that for % OC. Given that *B. constans* is regarded as a fertility indicator and generally is most abundant in organic carbon-rich hemicycles, we might expect it to more closely reflect fluctuations in % OC if organic productivity were the driving mechanism. However, it is possible that slight dissolution of *B. constans* in association with the minor diagenesis that attended formation of the Bridge Creek limestone beds (Ricken, 1994) modified relative abundance values to more closely follow variations in $CaCO_3$ content. Unfortunately the ecological affinities of *Tranolithus* spp. are not well know (Burns and Bralower, this volume).

In addition to the characteristics discussed above, each of the data sets shows variations in expression through the Bridge Creek that bear on the origin of bedding cyclicity. For example, Sageman et al. (1997) described variations in carbonate content and bed thickness trends from the lower to the upper Bridge Creek. Burns and Bralower (this volume) indicated that preservation was better in the upper part. Savrda (this volume) illustrated that the ORI cycles recognized in the lower part of Bridge Creek Member of the Pueblo core (and interpreted to reflect the precessional index) do not occur in the upper part. Thus, the lowest part of the Bridge Creek is characterized by a record that may reflect both amalgamation and dilution of cycles. The middle part (upper *N. juddi* and *W. devonense* Biozones) includes bedding couplets that suggest a 1:5 pattern (note two to three E1 cycles marked with *'s in Fig. 8), but this could not be confirmed by spectral analysis. Although E and P signals were detected in the spectral results from the upper part of the Bridge Creek, the 1:5 pattern is not apparent. Instead, a 1:2 or 1:3 bedding pattern becomes predominant.

*Analysis of Cycle Hierarchy*

Based on the spectral results we hypothesize that P, O, and

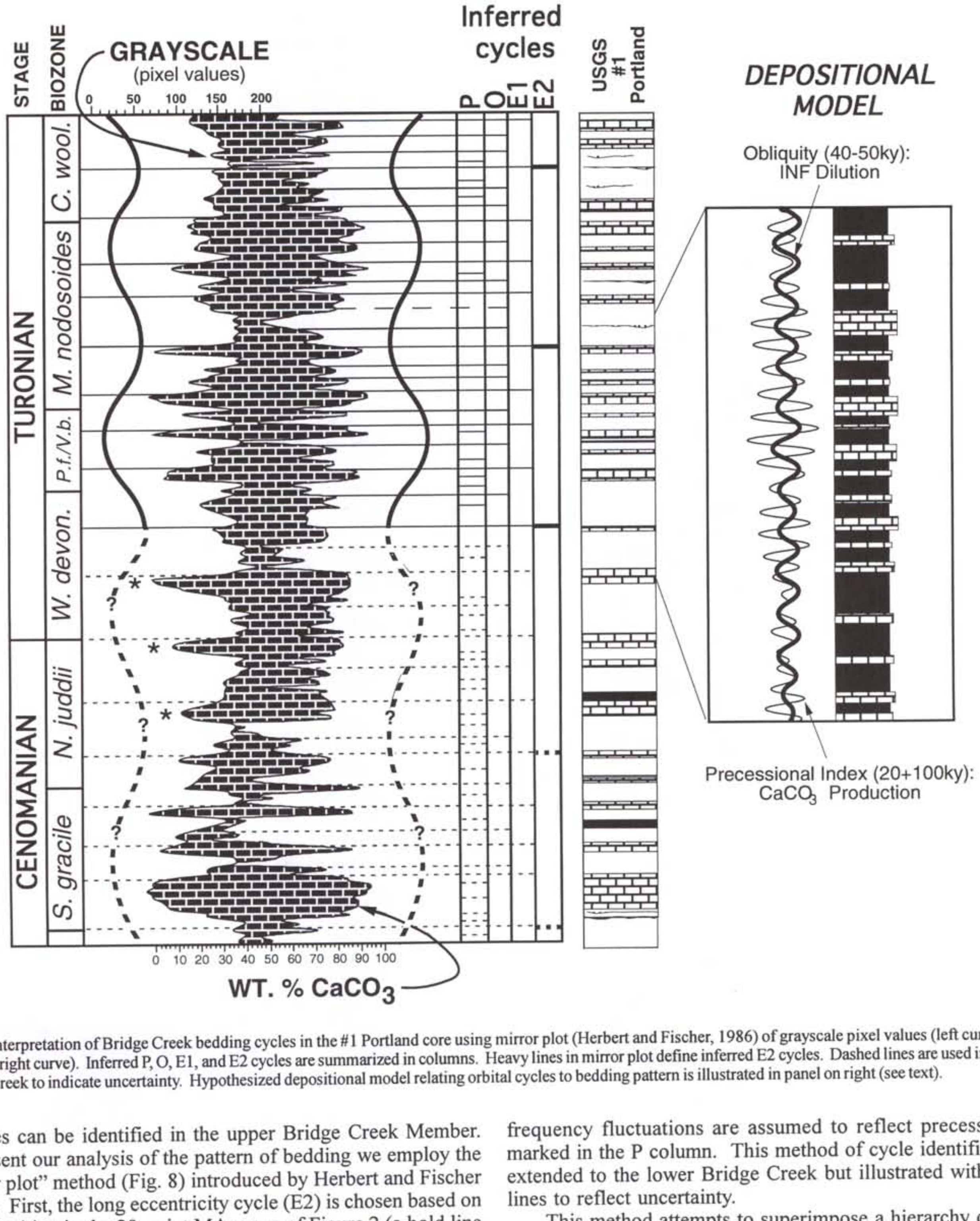


FIG. 8. Interpretation of Bridge Creek bedding cycles in the #1 Portland core using mirror plot (Herbert and Fischer, 1986) of grayscale pixel values (left curve) and % $CaCO_3$ (right curve). Inferred P, O, E1, and E2 cycles are summarized in columns. Heavy lines in mirror plot define inferred E2 cycles. Dashed lines are used in the lower Bridge Creek to indicate uncertainty. Hypothesized depositional model relating orbital cycles to bedding pattern is illustrated in panel on right (see text).

E cycles can be identified in the upper Bridge Creek Member. To present our analysis of the pattern of bedding we employ the "mirror plot" method (Fig. 8) introduced by Herbert and Fischer (1986). First, the long eccentricity cycle (E2) is chosen based on its recognition in the 20-point MA curve of Figure 2 (a bold line marks the E2 "envelop" and boundaries are placed in the E2 column for inferred cycles). Then, assuming that obliquity comprises a dominant signal, every limestone bed greater than about 10 cm is marked by a line on the right side of the mirror plot, extending from the $CaCO_3$ curve and ending in the O column. If the O signal represents about 40-50 ky, then approximately every other cycle would correspond to E1. The E1 cycles are thus delineated on the left side of Figure 8 (with lines extending from the gray-scale curve) and marked in the E1 column. Higher frequency fluctuations are assumed to reflect precession and marked in the P column. This method of cycle identification is extended to the lower Bridge Creek but illustrated with dashed lines to reflect uncertainty.

This method attempts to superimpose a hierarchy of cycles on the record of bedding. In the upper Bridge Creek this hierarchy explains the data fairly well. Although there are irregularities in the pattern (e.g., some E1 cycles correspond to two O cycles whereas others have three), this is to be expected given the variations in the orbital quasi-periods and resulting phase relationships among cycles. We extended this cycle hierarchy to the lower Bridge Creek using the same principles, but the lower interval does not follow the same pattern as clearly (Fig. 8). The characteristics of the lower Bridge Creek suggest more than

TABLE 5.- *MTM analysis of nannofossil data from the Bridge Creek Limestone.*

| Frequency (cycles/m) | Amplitude (Rel. Abund.) | Phase (degrees) | F-test (>90% only) | Period-kyr (0.6cm/kyr) | |
|---|---|---|---|---|---|
| *Biscutum constans* | | | | | |
| 0.1196 | 0.0185 | 154.49 | 5.1 | 1393.19 | |
| 0.5908 | 0.0119 | 37.4 | 4.8 | 282.09 | |
| 1.8237 | 0.0098 | 109.56 | 7.05 | **91.39** | *E1* |
| 2.6099 | 0.0026 | -146.9 | 3.65 | 63.86 | |
| 3.3667 | 0.0041 | 157.16 | 5.29 | 49.5 | |
| 4.3311 | 0.0038 | 74.02 | 4.42 | **38.48** | *O1* |
| 4.8535 | 0.002 | -137.86 | 3.57 | 34.34 | |
| 5.6616 | 0.0014 | -42.47 | 3.59 | 29.44 | |
| 6.2671 | 0.0011 | 145.5 | 3.98 | 26.59 | |
| 6.7676 | 0.0011 | -43.77 | 8.2 | **24.63** | *P2* |
| 7.4048 | 0.0006 | 136.12 | 4.09 | 22.51 | |
| 7.9981 | 0.0008 | -93.57 | 3.26 | **20.84** | *P1* |
| 8.9893 | 0.0003 | -167.72 | 3.18 | 18.54 | |
| 9.209 | 0.0003 | -110.11 | 4.06 | 18.1 | |
| *Zygodiscus* spp. | | | | | |
| 0.1147 | 0.012 | 135.48 | 3.76 | 1452.48 | |
| 0.5957 | 0.0096 | -63.5 | 7.19 | 279.78 | |
| 1.1987 | 0.0051 | -86.76 | 8.41 | 139.04 | |
| 1.6992 | 0.004 | 138.9 | 3.3 | **98.08** | *E1* |
| 2.3657 | 0.0052 | 30.27 | 9.61 | 70.45 | |
| 2.9663 | 0.0031 | -71.45 | 3.42 | 56.19 | |
| 3.4717 | 0.0028 | 116.26 | 5.11 | 48.01 | |
| 4.082 | 0.0034 | -74.5 | 7.34 | **40.83** | *O1* |
| 4.8999 | 0.002 | -80.63 | 4.76 | 34.01 | |
| 5.8228 | 0.0014 | 161.57 | 9.14 | 28.62 | |
| 6.8384 | 0.0007 | -67.92 | 3.59 | **24.37** | *P2* |
| 7.9004 | 0.0005 | 130.2 | 3.17 | **21.1** | *P1* |
| *Eiffellithus* spp. | | | | | |
| 0.5396 | 0.0063 | 21.29 | 8.73 | 308.9 | |
| 3.2178 | 0.0038 | 85.14 | 5.63 | **51.8** | *O2* |
| 3.9111 | 0.0023 | 14.95 | 5.27 | **42.61** | *O1* |
| 4.1748 | 0.0025 | -51.28 | 3.39 | 39.92 | |
| 4.4385 | 0.0024 | -176.5 | 4.38 | 37.55 | |
| 5.9106 | 0.0018 | 61.72 | 5.87 | 28.2 | |
| 7.3584 | 0.0009 | -88.77 | 3.13 | **22.65** | *P2* |
| 9.187 | 0.0003 | -149.49 | 16.52 | 18.14 | |
| 9.8731 | 0.0003 | -147.91 | 5.35 | 16.88 | |
| *Tranolithus* spp. | | | | | |
| 0.1367 | 0.0085 | 144.08 | 4.06 | 1219.04 | |
| 1.2647 | 0.0045 | -17.48 | 3.87 | 131.79 | |
| 2.124 | 0.0033 | -95.14 | 12.08 | 78.47 | |
| 3.2129 | 0.0052 | 85.13 | 4.07 | **51.87** | *O2* |
| 4.1113 | 0.0023 | 13.8 | 3.65 | **40.54** | *O1* |
| 4.773 | 0.0025 | 146.45 | 6.91 | 34.92 | |
| 5.2979 | 0.0023 | -13.45 | 8.12 | 31.46 | |
| 6.1255 | 0.0025 | 53.98 | 13.02 | 27.21 | |
| 7.2144 | 0.0017 | 96.26 | 8.73 | **23.1** | *P2* |

*1. Only frequencies with F-tests above the 90% confidence level are shown.*

*2. Period values were calculated using S = 0.6 cm/kyr. Frequency values close to the dominant orbital cycles are designated as E1, E2, etc., and their period values are printed in bold.*

simple variance in sedimentation rates. Some limestone beds may be amalgamated and others missing entirely. Sageman et al. (1997) concluded that changes in the production and (or) preservation of OC related to OAE II, the influence of aperiodic ash fall, and changes in detrital flux related to a transgressive event, altered the pattern of bedding thicknesses in the lower Bridge Creek sufficiently to modify the preservation of orbital influence. Extending the cycle hierarchy from the upper to the lower Bridge Creek thus provides a framework within which variations in the linkage between climate and the depositional system can be better understood.

### *Origin Of Bedding Cyclicity*

As pointed out by Ricken (1994), LaFerriere et al. (1987), Arthur and Dean (1991), and Elder et al. (1994), the development of bedding cycles in Cretaceous rocks of the Western Interior basin reflects a highly sensitive depositional system. This system was influenced by minor changes in relative sea level and climate that periodically modulated the fluxes of organic matter, carbonate, and detrital material to the basin. At times it was also sensitive to the aperiodic input of volcanic ash. The preservation of bedding cycles that record orbital influence sufficiently to allow spectral analysis is limited to the highstand of a relative sea-level cycle that occurred near peak marine flooding of the basin (Fig. 7).

The results of spectral analyses for this highstand interval suggest that the complex pattern of the Bridge Creek bedding couplets may reflect constructive and destructive interference of separate orbital cycles that preferentially influenced different parts of the depositional system (Sageman et al., 1997). As a result of the meridional configuration of the seaway, the basin spanned multiple climate zones, and was thus subject to latitudinal variations in climate forcing. The major control of bedding cycles is thought to be dilution by detrital input (e.g., Arthur et al., 1985; Barron et al., 1985; Pratt et al., 1993). Variations in precipitation in the northern part of the seaway, which probably played a significant role in the dilution process, would have been particularly sensitive to obliquity (Park and Oglesby, 1991, 1994). However, if precession produced the dominant effect on climate at lower latitudes, as is predicted, it may have influenced carbonate productivity in the manner suggested by Eicher and Diner (1985, 1989) and superimposed variations in carbonate flux on dilution cycles within the basin. The relative influence of the northern and southern climate belts in the seaway would determine the degree of cycle mixing. Phase relations would cause positive and negative interference during cycle development where mixing was strong, resulting in a complex bedding pattern (this interpretation may explain some of the F-test results interpreted to represent interference beats).

This depositional model is illustrated on the right side of Figure 8. The formation of limestone beds is modeled as the product of clastic dilution (represented by the bold "O" or obliquity curve, which increases to the right) and carbonate input (represented by the thin "P" or precessional index curve, which increases to the right). Only where O is low can P produce thick limestone beds (in some cases by amalgamating two P cycles). When O is high, P may produce a small bed or no bed at all depending on the modulation of E1 and E2 (Fig. 8). This model produces a 1:2 or 1:3 pattern of bedding couplets like that observed in the upper Bridge Creek, and the long term variation it creates (E2 scale) also matches the observations from the Portland core (Fig. 8). This model implies that the onset of bedding cyclicity in the lower Bridge Creek was dominated by a southern (precessional) influence, but that through time the northern (obliquity) influence became more dominant. Sageman et al. (1997) hypothesized that this shift was caused by an Early Turonian cooling event precipitated by the global burial of carbon during OAE II, as was suggested by Arthur et al. (1988).

The depositional model is supported by the interpretation of decoupling between the % $CaCO_3$ record and % OC record, which suggests that the dominant control on carbonate production was unrelated or not entirely related to the controls on OC burial. One possibility is that OC preservation solely depended on stratification intensity, and thus was closely tied to runoff volume. But carbonate content, being the net product of dilution (due to run-off) and carbonate productivity (controlled by Tethyan surface waters), had a more complex origin. Another possibility is that OC burial was strongly influenced by production of noncalcareous plankton (e.g., diatoms), and these taxa were more sensitive to fluctuations in nutrient supply within the seaway. In this scenario the correlation between ORI and %OC in the upper Bridge Creek would reflect increases in river-borne nutrients, productivity among noncalcareous plankton, and organic loading of substrates leading to lower oxygen levels in bottom waters. The low % OC levels of clay-rich hemicycles in the lower Bridge Creek may indicate that nutrient supply was too low to stimulate excess productivity among the noncalcareous plankton. As a result, OC flux to the sediment would have been insufficient to drive pore waters anoxic. This allowed more infauna to colonize, further reducing preserved OC levels. The increase in relative abundance of the fertility indicator *B. constans* from the lower to the upper Bridge Creek provides support for this interpretation (see also discussion in Burns and Bralower, this volume).

## CONCLUSIONS

The Bridge Creek Limestone has long been interpreted as a product of orbital influences (Fischer, 1980), although determining of the periodicity and depositional mechanisms responsible for the cycles has been difficult. Detailed quantitative analysis of complementary paleoecological and geochemical data, however, helps to reveal the complexities of orbital expression in the Bridge Creek record. Understanding these complexities illuminates the paleoenvironmental history of the Western Interior basin.

Our study was made possible by new high-resolution $^{40}Ar/^{39}Ar$ radiometric dates, which improve estimates of age-depth relationships for the Bridge Creek Limestone. These estimates allow meaningful application of spectral analyses. Spectral analysis of three complementary analytical records from the Portland core, including lithologic data (weight % $CaCO_3$, weight % OC, and optical densitometry of core photographs), ichnologic data (maximum burrow diameter, oxygen-related ichnocoenoses), and nannofossil data (species abundance trends), indicate the presence of obliquity and precessional index signals in the upper Bridge Creek.

Analysis of the spectral results from multiple complementary data sets suggests a depositional model for the bedding couplets that combines the dilution and productivity mechanisms. Obliquity, through its effect on high-latitude precipitation, is thought to predominantly influence dilution processes whereas the precessional index mainly controls changes in carbonate productivity through its effect on evaporation and nutrient upwelling in the Tethyan realm. The two influences mix in the shallow Western Interior basin and result in constructive and destructive interference, producing a complex bedding pattern. In addition, variations in cycle expression through the Bridge Creek provided a high-resolution record of changes in the depositional system, revealing intervals of unusual condensation and aperiodic dilution. Some of these corroborate and help refine interpretations of relative sea level history for the study interval.

Comparison of %OC data with trends in trace fossils and nannofossils, which act as proxies for benthic redox conditions and primary production, respectively, suggest that organic matter production and preservation were decoupled from carbonate production. The recognition that $CaCO_3$ production and OC production may fluctuate in phase, out of phase, or antithetically probably reflects changes in the ecological structure of the primary producer community and the different responses of taxonomic groups to changing climatic and oceanographic conditions.

The interpretative model presented herein is based on (1) determination of patterns in Bridge Creek bedding cycles using a quantitative method (spectral analysis), and extension of that pattern to parts of the section where spectral analysis is not possible, and (2) analysis of multiple data sets reflecting different components of the depositional system. The interpretative model provides a reasonable explanation for the bedding patterns observed throughout the Bridge Creek, and attempts to synthesize the observations of past workers (Pratt, 1984; Arthur et al., 1985; Barron et al., 1985; Eicher and Diner, 1985, 1989; Watkins, 1989; Pratt et al., 1993) into a comprehensive scheme. Finally, the model highlights the relative importance of sea level, paleogeography and latitudinal climate belts, the hydrologic cycle, nutrient flux, and marine primary productivity in preserving Milankovitch orbital cycles in the Western Interior rock record. The development of these cycles within the highstand phase of the Greenhorn Cyclothem represented a stratigraphic "window

## REFERENCES


Arthur, M. A., Dean, W. E., Bottjer, D., and Scholle, P. A., 1984, Rhythmic bedding in Mesozoic-Cenozoic pelagic carbonate sequences; the primary and diagenetic origin of Milankovitch-like cycles, *in* Berger, A., Imbrie, J., Hays, J. D, Kukla, G., and Saltzman, B., eds., Milankovitch and Climate, pt. 1: Amsterdam, Reidel Publishing Company, p. 191-222.

Arthur, M. A., Dean, W. E., Pollastro, R., Scholle, P. A., and Claypool, G. E., 1985, A comparative geochemical study of two transgressive pelagic limestone units, Cretaceous Western Interior basin, U.S., *in* Pratt, L. M., Kauffman, E. G., and Zelt, F. B., eds., Fine-grained Deposits and Biofacies of the Cretaceous Western Interior Seaway: Evidence of Cyclic Sedimentary Processes, Field Trip Guidebook No. 4: Tulsa, Society of Economic Paleontologists and Mineralogists, p. 16-27.

Arthur, M. A., Dean, W. E., and Pratt, L. M., 1988, Geochemical and climatic effects of increased marine organic carbon burial at the Cenomanian/Turonian boundary: Nature, v. 335, p. 714-717.

Arthur, M. A., and Dean, W. E., 1991, An holistic geochemical approach to cyclomania: Examples from Cretaceous pelagic limestone sequences, *in* Einsele, G., Ricken, W., and Seilacher, A., eds., Cycles and Events in Stratigraphy: Berlin, Springer Verlag, p. 126-166.

Arthur, M.A. and Sageman, B.B., 1994, Marine Black Shales: A Review of Depositional Mechanisms and Environments of Ancient Deposits: Annual Reviews of Earth & Planetary Science, v. 22, pp. 499-552.

Barron, E. J., Arthur, M. A., and Kauffman, E. G., 1985, Cretaceous rhythmic bedding sequences: A plausible link between orbital variations and climate: Earth Planetary Science Letters, v. 72, p. 327-340.

Berger, A., 1978, Long-term variations of daily insolation and Quaternary climate change: Journal of Atmospheric Science, v. 35, p. 2362-2367.

Berger, A., 1984, Accuracy and frequency stability of the Earth's orbital elements during the Quaternary, *in* Berger, A., Imbrie, J., Hays, J. D., Kukla, G., and Saltzman, B., eds., Milankovitch and Climate, pt. 1: Amsterdam, Reidel Publishing Company, p. 3-40.

Berger, A., Loutre, M. F., and Dehant, V., 1989, Astronomical frequencies for pre-Quaternary palaeoclimate studies: Terra Nova, v. 1, p. 474-479.

Berger, A., Loutre, M. F., and Laskar, J., 1992, Stability of the astronomical frequencies over the Earth's history for paleoclimate studies: Science, v. 255, p. 560-566.

Bralower, T. J., 1988, Calcareous nannofossil biostratigraphy and assemblages of the Cenomanian-Turonian boundary interval: Implications for the origin and timing of anoxia: Paleoceanography, v. 3, p. 275-316.

Caldwell, W. G. E. and Kauffman, E. G., eds., 1993, Evolution of the Western Interior Basin: St. John's, Geological Association of Canada Special Paper 39, 680 p.

Caputo, M., Peterson, J. and Franczyk, K., eds., 1994, Mesozoic Systems of the Rocky Mountain Region: Tulsa, Society of Economic Paleontologists and Mineralogists Special Publication, 536 p.

Cobban, W. A., 1984, Mid-Cretaceous ammonite zones, Western Interior, United States: Bulletin Geological Society Denmark, v. 33, p. 71-89.

Cobban, W. A., 1985, Ammonite record from Bridge Creek Member of Greenhorn Limestone at Pueblo Reservoir State Recreation Area, Colorado, *in* Pratt, L. M. Kauffman, E. G., and Zelt, F. B., eds., Fine-grained Deposits and Biofacies of the Cretaceous Western Interior Seaway: Evidence of Cyclic Sedimentary Processes, Field Trip Guidebook No. 4: Tulsa, Society of Economic Paleontologists and Mineralogists, p. 135-138.

Cobban, W. A., and Scott, R. W., 1972, Stratigraphy and Ammonite Fauna of the Graneros Shale and Greenhorn Limestone Near Pueblo, Colorado: Washington, D.C., U.S. Geological Survey Professional Paper 645, p. 1-108.

Dean, W. E., and Arthur, M. A., 1994, The Cretaceous Western Interior Seaway Drilling Project, An overview (abs.): American Association of Petroleum Geologists Annual Meeting, Abstracts with Program, v. 3, p. 134.

Eicher, D. L., and Diner, R., 1985, Foraminifera as indicators of water mass in the Cretaceous Greenhorn Sea, Western Interior, *in* Pratt, L. M., Kauffman, E. G., and Zelt, F. B., eds., Fine-grained Deposits and Biofacies of the Cretaceous Western Interior Seaway: Evidence of Cyclic Sedimentary Processes, Field Trip Guidebook No. 4: Tulsa, Society of Economic Paleontologists and Mineralogists, p. 60-71.

Eicher, D. L., and Diner, R., 1989, Origin of the Cretaceous Bridge Creek cycles in the Western Interior, United States: Palaeogeography, Palaeoclimatology, and Palaeoecology, v. 74, p. 127-146.

Eicher, D. L., and Diner, R., 1991, Environmental factors controlling Cretaceous limestone-marlstone rhythms, *in* Einsele, G., Ricken, W., and Seilacher, A., eds., Cycles and Events in Stratigraphy: Berlin, Springer Verlag, p. 79-93.

Elder, W. P., 1985, Biotic patterns across the Cenomanian-Turonian extinction boundary near Pueblo, Colorado, *in* Pratt, L. M., Kauffman, E. G., and Zelt, F. B., eds., Fine-grained Deposits and Biofacies of the Cretaceous Western Interior Seaway: Evidence of Cyclic Sedimentary Processes, Field Trip Guidebook No. 4: Tulsa, Society of Economic Paleontologists and Mineralogists, p. 157-169.

Elder, W. P., Gustason, E. R., and Sageman, B. B., 1994, Basinwide correlation of parasequences in the Greenhorn Cyclothem, Western Interior, U.S.: Geological Society of America Bulletin, v. 106, p. 892-902.

Engleman, E. E., Jackson, L. L., Norton, D. R., and FISCHER, A. G., 1985, Determination of carbonate carbon in geological materials by coulometric titration: Chemical Geology, v. 53, p. 125-128.

Erba, E., Castradori, D., Guasit, G., and Ripepe, M., 1992, Calcareous nannofossils and Milankovitch cycles: The example of the Albian Gault Clay Formation (southern England): Palaeogeography, Palaeoclimatology, and Palaeoecology, v. 93, p. 47-69.

Erba, E., and Premoli-Silva, I., 1994, Orbitally driven cycles in trace fossil distribution from the Piobbico core (late Albian, central Italy), *in* deBoer, P. L., and Smith, D. G., eds., Orbital Forcing and Cyclic Sequences: International Association of Sedimentologists Special Publication 19, Oxford, Blackwell Scientific Publications, p. 219-225.

Fischer, A. G., 1980, Gilbert-bedding rhythms and geochronology, in Yochelson, E. L., ed., The Scientific Ideas of G. K. Gilbert: Boulder, Geological Society of America Special Paper 183, p. 93-104.

Fischer, A. G., Herbert, T., and Premoli-Silva, I., 1985, Carbonate bedding cycles in Cretaceous pelagic and hemipelagic sediments, *in* Pratt, L. M., Kauffman, E. G., and Zelt, F. B., eds., Fine-grained Deposits and Biofacies of the Cretaceous Western Interior Seaway: Evidence of Cyclic Sedimentary Processes, Field Trip Guidebook No. 4: Tulsa, Society of Economic Paleontologists and Mineralogists, p. 1-10.

Gilbert, G. K., 1895, Sedimentary measurement of geologic time: Geology, v. 3, p. 121-127.

Glancy, T. J., Jr., Arthur, M. A., Barron, E. J., and Kauffman, E. G., 1993, A paleoclimate model for the North American Cretaceous (Cenomanian-

Turonian) epicontinental sea, *in* Caldwell, W. G. E., and Kauffman, E. G., eds., Evolution of the Western Interior Basin: St. John's, Geological Association of Canada Special Paper 39, p. 219-242.

Haq, B. V., Hardenbol, J., and Vail, P. R., 1987, Chronology of fluctuating sea levels since the Triassic (250 million years ago to present): Science, v. 235, p. 1159-1167.

Herbert, T. D., and Fischer, A. G., 1986, Milankovitch climatic origin of mid-Cretaceous black shale rhythms in central Italy: Nature, v. 321, p. 739-743.

Jordan, T. E., 1981, Thrust loads and foreland basin evolution, Cretaceous, western United States: American Association of Petroleum Geologists Bulletin, v. 65, p. 2506-2520.

Kauffman, E. G., 1977, Geological and biological overview: Western Interior Cretaceous Basin: Mountain Geologist, v. 13, p. 75-99.

Kauffman, E. G., 1984, Paleobiogeography and evolutionary response dynamic in the Cretaceous Western Interior Seaway of North America, *in* Westermann, G. E. G., ed., Jurassic-Cretaceous Biochronology and Paleogeography of North America: St. John's, Geological Association of Canada Special Paper 27, p. 273-306.

Kauffman, E. G., 1995, Global change leading to biodiversity crisis in a greenhouse world: The Cenomanian-Turonian (Cretaceous) mass extinction. Effects of past global change on life, *in* Studies in Geophysics: Washington, D.C., National Academy Press, p. 47-71.

Kauffman, E. G., Sageman, B. B., Elder, W. P., Kirkland, J. I., and Villamil, T., 1993, Cretaceous molluscan biostratigraphy and biogeography, Western Interior Basin, North America, *in* Caldwell, W. G. E., and Kauffman, E. G., eds., Evolution of the Western Interior Basin: St. John's, Geological Association of Canada Special Paper 39, p. 397-434.

Kennedy, W. J., and Cobban, W. A., 1991, Stratigraphy and interregional correlation of the Cenomanian-Turonian transition in the Western Interior of the United States near Pueblo, Colorado, a potential boundary stratotype for the base of the Turonian stage: Newsletter of Stratigraphy, v. 24(1/2), p. 1-33.

Laferriere, A. P., Hattin, D., and Archer, A. W., 1987, Effects of climate, tectonics and sea-level changes on rhythmic bedding patterns in the Niobrara Formation (Upper Cretaceous), U.S., Western Interior: Geology, v. 15, p. 233-236.

Ludvigson, G. A., Witzke, B. J., Gonzalez, L. A., Hammond, R. H., and Plocher, O. W., 1994, Sedimentology and carbonate geochemistry of concretions from the Greenhorn Marine Cycle (Cenomanian-Turonian), eastern margin of the Western Interior Seaway, *in* Shurr, G. W., Ludvigson, G. A., and Hammond, R. H., eds., Perspectives on the Eastern Margin of the Cretaceous Western Interior Basin: Boulder, Geological Society of America Special Paper 287, p. 145-174.

Obradovich, J., 1993, A Cretaceous time scale, *in* Caldwell, W. G. E., and Kauffman, E. G., eds., Evolution of the Western Interior Basin: St. John's, Geological Association of Canada Special Paper 39, p. 379-396.

Obradovich, J. D., and Cobban, W. A., 1975, A time-scale for the Late Cretaceous of the Western Interior of North America, *in* Caldwell, W. G. E., ed., The Cretaceous System in the Western Interior of North America: St. John's, Geological Association of Canada Special Paper 13, p. 31-54.

Park, J., and Herbert, T. D., 1987, Hunting for paleoclimatic periodicities in a geologic time series with an uncertain time scale: Journal of Geophysical Research, v. 92, p. 14027-14040.

Park, J., and Oglesby, R. J., 1991, Milankovitch rhythms in the Cretaceous: A GCM modelling study: Palaeogeography, Palaeoclimatology, and Palaeoecology (Global and Planetary Change), v. 90, p. 329-355.

Park, J., and Oglesby, R. J., 1994, The effect of orbital cycles on Late and Middle Cretaceous climate: A comparative general circulation model study, *in* deBoer, P. L., and Smith, D. G., eds., Orbital Forcing and Cyclic Sequences: International Association of Sedimentologists Special Publication 19, Oxford, Blackwell Scientific Publications, p. 509-529.

Pratt, L. M., 1984, Influence of paleoenvironmental factors on the preservation of organic matter in middle Cretaceous Greenhorn Formation near Pueblo, Colorado: American Association of Petroleum Geologists Bulletin, v. 68, p. 1146-1159.

Pratt, L. M., 1985, Isotopic studies of organic matter and carbonate in rocks of the Greenhorn marine cycles, *in* Pratt, L. M., Kauffman, E. G., and Zelt, F. B., eds., Fine-grained Deposits and Biofacies of the Cretaceous Western Interior Seaway: Evidence of Cyclic Sedimentary Processes, Field Trip Guidebook No. 4: Tulsa, Society of Economic Paleontologists and Mineralogists, p. 38-48.

Pratt, L. M., Kauffman, E. G., and Zelt, F. B., eds., 1985, Fine-grained Deposits and Biofacies of the Cretaceous Western Interior Seaway: Evidence of Cyclic Sedimentary Processes, Field Trip Guidebook No. 4: Tulsa, Society of Economic Paleontologists and Mineralogists, 249 p.

Pratt, L. M., Arthur, M. A., Dean, W. E., and Scholle, P. A., 1993, Paleoceanographic cycles and events during the Late Cretaceous in the Western Interior Seaway of North America, *in* Caldwell, W. G. E., and Kauffman, E. G., eds., Evolution of the Western Interior Basin: St. John's, Geological Association of Canada Special Paper 39, p. 333-354.

Ricken, W., 1991, Variation of sedimentation rates in rhythmically bedded sediments - distinction between depositional types, *in* Einsele, G., Ricken, W., and Seilacher, A., eds., Cycles and Events in Stratigraphy: Berlin, Springer-Verlag, p. 167-187.

Ricken, W., 1994, Complex rhythmic sedimentation related to third-order sea-level variations: Upper Cretaceous, Western Interior Basin, USA, *in* deBoer, P. L., and Smith, D. G., eds., Orbital Forcing and Cyclic Sequences: International Association of Sedimentologists Special Publication 19, Oxford, Blackwell Scientific Publications, p. 167-193.

Roth, P. H., and Bowdler, J. L., 1981, Middle Cretaceous calcareous nannoplankton biogeography and oceanography of the Atlantic Ocean: Tulsa, Society of Economic Paleontologists and Mineralogists Special Publication 32, p. 517-546.

Roth, P. H. and Krumbach, K. R., 1986, Middle Cretaceous nannofossil biogeography and preservation in the Atlantic and Indian Oceans: Implications for paleoceanography: Marine Micropaleontology, v. 10, p. 235-266.

Sageman, B. B., 1996, Lowstand Tempestites: Depositional model for Cretaceous skeletal limestones, Western Interior, U.S.: Geology, v. 24, p. 888-892.

Sageman, B. B., 1991, High-resolution event stratigraphy, carbon geochemistry, and paleobiology of the Upper Cenomanian Hartland Shale Member (Cretaceous), Greenhorn Formation, Western Interior, U.S.: Unpublished Ph.D. Dissertation, University of Colorado, Boulder, 572 p.

Sageman, B. B., Rich, J., Arthur, M. A., Birchfield, G. E., and Dean, W. E., 1997, Evidence For Milankovitch periodicities in Cenomanian-Turonian lithologic and geochemical cycles, Western Interior U.S., Journal of Sedimentary Research, v. 67, p. 285-301.

Savrda, C. E., and Bottjer, D. J., 1991, Oxygen-related biofacies in marine strata: An overview and update, *in* Tyson, R. V., and Pearson, T. H., eds., Modern and Ancient Continental Shelf Anoxia: London, Geological Society of London Special Publication 58, p. 201-220.

Savrda, C. E., and Bottjer, D. J., 1994, Ichnofossils and ichnofabrics in rhythmically bedded pelagic/hemi-pelagic carbonates: Recognition and evaluation of benthic redox and scour cycles, *in* deBoer, P. L., and Smith, D. G., eds., Orbital Forcing and Cyclic Sequences: International Association of Sedimentologists Special Publication 19, Oxford, Blackwell Scientific Publications, p. 195-210.

Schlanger, S. O., Arthur, M. A., Jenkyns, H. C., and Scolle, P. A., 1987, The Cenomanian-Turonian Oceanic Anoxic Event, I. Stratigraphy and distribution of organic carbon-rich beds and the marine $\delta^{13}C$ excursion, *in* Brooks, J., and Fleet, A. J., eds., Marine Petroleum Source Rocks: London, Geological Society of London Special Publication 26, p. 371-399.

Schwarzacher, W., and Fischer, A. G., 1982, Limestone-shale bedding and perturbations of the earth's orbit, *in* Einsele, G., Ricken, W., and Seilacher, A., eds., Cyclic and Event Stratification: Berlin, Springer-Verlag, p. 72-95.

Thomson, D. J., 1982, Spectrum estimation and harmonic analysis: Institute of Electrical and Electronics Engineers (IEEE), Proceedings, v. 70, p. 1055-1096.

Tyson, R. V., 1987, The genesis and palynofacies characteristics of marine pertroleum source rocks, *in* Brooks, J., and Fleet, A. J., eds., Marine Petroleum Source Rocks: London, Geological Society of London Special Publication 26, p. 47-67.

Upchurch, G.R., and Wolfe, J.A., 1993, Cretaceous vegetation of the Western Interior and adjacent regions of North America, *in* Caldwell, W. G. E., and Kauffman, E. G., eds., Evolution of the Western Interior Basin: St. John's, Geological Association of Canada Special Paper 39, p. 243-282.

Van Wagoner, J. C., Posimentier, H. W., Mitchum Jr., R. M., Vail, P. R., Sarg, J. F., Loutit, T. S., and Hardenbol, J., 1988, An overview of the fundamentals of sequence stratigraphy and key definitions, *in* Wilgus et al., eds., Sea-Level Changes: An Integrated Approach: Tulsa, Society of Economic Paleontologists and Mineralogists Special Publication 42, p. 39-46.

Watkins, D. K., 1985, Biostratigraphy and paleoecology of nannofossils in the Greenhorn marine cycle, *in* Pratt, L. M., Kauffman, E. G., and Zelt, F. B., eds Fine-grained Deposits and Biofacies of the Cretaceous Western Interior Seaway: Evidence of Cyclic Sedimentary Processes, Field Trip Guidebook No. 4: Tulsa, Society of Economic Paleontologists and Mineralogists, p. 151-156.

Watkins, D. K., 1989, Nannoplankton productivity fluctuations and rhythmically bedded pelagic carbonates of the Greenhorn Limestone (Upper Creatceous): Palaeogeography, Palaeoclimatology, and Palaeoecology, v. 74, p. 75-86.

Watkins, D. K., Bralower, T. J., Covington, J. M., and Fisher, C. G., 1993, Biostratigraphy and paleoecology of the upper Cretaceous calcareous nannofossils in the Western Interior Basin, North America, *in* Caldwell, W. G. E., and Kauffman, E. G., eds., Evolution of the Western Interior Basin: St. John's, Geological Association of Canada Special Paper 39, p. 521-538.

Witzke, B. J. and Ludvigson, G. A., 1994, The Dakota Formation in Iowa and the type area, *in* Shurr, G. W., Ludvigson, G. A., and Hammond, R. H., eds., Perspectives on the Eastern Margin of the Cretaceous Western Interior Basin: Boulder, Geological Society of America Special Paper 287, p. 43-78.